2015

CALIBRATION, VERIFICATION, AND DIAGNOSIS OF A SEASON-AHEAD DROUGHT PREDICTION MODEL: LIMITS TO PREDICTABILITY IN CENTRAL TEXAS

Jonathan Witham
Michigan Technological University, jdwitham@mtu.edu

CALIBRATION, VERIFICATION, AND DIAGNOSIS OF A SEASON-AHEAD DROUGHT PREDICTION MODEL: LIMITS TO PREDICTABILITY IN CENTRAL TEXAS

By

Jonathan D. Witham

A THESIS

Submitted in partial fulfillment of the requirements for the degree of

MASTER OF SCIENCE

In Environmental Engineering

MICHIGAN TECHNOLOGICAL UNIVERSITY

2015

This thesis has been approved in partial fulfillment of the requirements for the Degree of MASTER OF SCIENCE in Environmental Engineering.

Department of Civil and Environmental Engineering

Thesis Advisor: *Dr. David W. Watkins, Jr.*

Committee Member: *Dr. Alex S. Mayer*

Committee Member: *Dr. Joseph W. Wagenbrenner*

Department Chair: *Dr. David W. Hand*

To my loving family

Table of Contents

List of Figures

List of Tables

Preface

The text of this thesis was written by the author, with editing and technical assistance provided by adviser Dr. David Watkins, Jr., and committee members Drs. Alex Mayer and Joseph Wagenbrenner.

CH2M HILL generated the soil parameter file, vegetation parameter file, elevation parameter file, flow direction file, and fraction file which are used as inputs to the Variable Infiltration Capacity and Routing models presented in this thesis. The author modified these files appropriately for this research. These files are provided in the "01Model" folder in the supplemental materials.

Brian Zimmerman provided the list of analog years given in Appendix H, as part of his graduate research at the University of Wisconsin Madison. Mr. Zimmerman also generated the hindcast meteorological forcings files. These files are provided in the "01Model" folder in the supplemental materials.

Dr. Pengfei Xue and Chenfu Huang created the seasonal looping script for generating seasonal hindcasts over the historical record, with appropriate modifications applicable to this research made by the author. This script is provided in the "02External_Scripts" folder in the supplemental materials.

The scripts "latlon.c" and "aggregate_metdata.c" included in the "02External_Scripts" folder in the supplemental materials were created at the University of Washington as post-processing tools for the Variable Infiltration Capacity model, and are open source. The "aggregate_metdata.c" script was modified appropriately by the author for this research.

Acknowledgements

I would like to acknowledge my adviser, Dr. David Watkins, Jr., for his expertise, teaching, patience, and willingness to teach and guide me in the field of water resources engineering. I know how much work he balances, and I am truly grateful for his personal attention to my work and care. I also acknowledge my committee members, Drs. Alex Mayer and Joseph Wagenbrenner, for their guidance and suggestions, as well as review of this thesis.

I also acknowledge those who collaborated with me on this project, including Dr. Paul Block, Brian Zimmerman, and Matthew Grzegorzewski at the University of Wisconsin Madison; Laura Borgeau-Chavez and Colin Brooks at the Michigan Tech Research Institute; Dr. Bradfield Lyon at Columbia University; and Ron Anderson at the Lower Colorado River Authority. Without their contributions to research, analysis, data provision, and hard work, my work would not have been possible.

To those who helped me with scripting processes, I thank Dr. Pengfei Xue, Chenfu Huang, and my good friends Brandon Gafford and Chloe Sult. Without their computer programming knowledge, I would not have been able to make analyses so efficiently. I also thank Dr. Ann Mclean who helped me in the soil processing analysis.

I thank my God and Savior Jesus Christ, for giving me the ability to understand all He has created, and to steward His creation in order to care for His people.

This research was funded by the National Oceanic and Atmospheric Administration Climate Program Office Sectoral Application's Research Program (# NA130OAR4310126).

Abbreviations

ASCII	American Standard Code for Information Interchange
b_{infilt}	Shape parameter of the infiltration capacity curve
cfs	Cubic feet per second
Co-op	Cooperative-observer
CRBU	Lake Buchanan station
CRTR	Lake Travis station
CRTR-CRBU	The sub-basin below CRBU and above CRTR
DEM	Digital Elevation Model
Ds	Fraction of Ds_{max} where non-linear baseflow is observed
Ds_{max}	Maximum baseflow in the bottommost soil layer
DSS	Decision Support System
ENSO	El Niño Southern Oscillation
ESP	Ensemble Streamflow Prediction
GCC	GNU (GNU's Not Unix) Compiler Collection
GCM	General Circulation Model
GIS	Geographic Information System
GRG	Generalized Reduced Gradient
HUC	Hydrologic Unit Code
JASO	July, August, September, and October
LBJ	Lyndon B. Johnson reservoir/basin
LCRA	Lower Colorado River Authority
LSM	Land Surface Model

MAMJ	March, April, May, and June
MOCUM-UA	Multi-Objective Complex Evolution method
MSCC	Multisite Cascading Calibration method
MTRI	Michigan Tech Research Institute
MUID	Map Unit Identification
NAO	North Atlantic Oscillation
NASA	National Aeronautics and Space Administration
NCAR	National Center for Atmospheric Research
NCDC	National Climatic Data Center
NCEP	National Centers for Environmental Prediction
NDJF	November, December, January, and February
NLDAS	North American Land Data Assimilation System
NOAA	National Oceanic and Atmospheric Administration
NSE	Nash-Sutcliffe Efficiency
NWP	Numerical Weather Prediction
PCSWMM	PC Stormwater Management Model
PDO	Pacific Decadal Oscillation
PDSI	Palmer Drought Severity Index
PRISM	Parameter-elevation Relationships on Independent Slopes Model
RCM	Regional Climate Model
SRTC	Sensitivity-based Radio Tuning Calibration tool
SSDP	Sampling Stochastic Dynamic Programming
SSURGO	Soil Survey Geographic database
STATSGO	State Soil Geographic database

SVATS	Soil-vegetation-atmosphere transfer scheme
SYMAP	Synergraphic Mapping System
USDA	United States Department of Agriculture
VIC	Variable Infiltration Capacity model
Ws	Maximum soil moisture fraction where non-linear baseflow is observed in the bottommost soil layer

Abstract

The Variable Infiltration Capacity (VIC) land surface hydrology model was calibrated and verified for prediction of naturalized flows into the Highland Lakes system in central Texas. Using seasonal climate forecasts downscaled to daily precipitation, maximum and minimum temperatures, and wind speeds, the VIC model was run to generate ensemble inflow hindcasts for two seasons – March through June and July through October – corresponding to the period of 1960 through 2010. A diagnosis of the seasonal hindcast results determined that inflows are not as heavily influenced by the physical soil moisture state as expected, and that variability in statistical precipitation downscaling can combine with hydrologic model errors to degrade the skill in streamflow forecasts. Recommendations are made for future work to improve forecast skill.

Chapter 1. Introduction

1.1. An Overview of Drought

Drought is a growing concern across the United States and the world, especially in regions susceptible to variable weather patterns and climates (Hallack-Alegria and Watkins 2005; Seager et al. 2015; Trnka et al. 2003). A standard definition of drought is a lack of precipitation in a region, extending for a season or longer time period, which impairs the ability to meeting water demands (Wilhite 1992b). In practice, defining drought is not simple (Dracup et al. 1980b; McKee et al. 1993; Wilhite and Glantz 1985), as drought is defined differently according to the sectors and regions it affects. There are four categories to describe drought type, including meteorological, hydrological, agricultural, and socioeconomic (Mozny et al. 2012; Tabari et al. 2013; Wilhite and Glantz 1985). Meteorological drought is associated with the lack of precipitation when compared to the norm for a geographic region. Climatic variations and atmospheric circulation patterns, including wind patterns, sea surface temperatures, and oceanic oscillation events like the El Niño Southern Oscillation (ENSO), North Atlantic Oscillation (NAO), and Pacific Decadal Oscillation (PDO), often contribute to the initiation and termination of droughts. Hydrological drought represents the effects of a lack of rainfall on surface waters and managed waters, causing lower water levels in rivers and reservoirs, for example (Nalbantis and Tsakiris 2009; Ryu et al. 2014; Tabari et al. 2013; Wilhite 1992b). A river basin is considered to be in hydrological drought when the stream discharge is measured below a discharge threshold for a period of time. However, the time period and discharge threshold varies between basins and is subject to

the water managers of the basin to define (Wilhite and Glantz 1985). Agricultural drought examines the lack of water in the form of increased evapotranspiration and soil-water deficits, which can affect crop yield. Lastly, socioeconomic drought examines the supply and demand of resources affected during drought, such as energy, crops, food stuffs, and water supply. The main focus of the study in this thesis is on hydrological drought.

Drought is also difficult to define based on its prolonged onset from variable environmental conditions. Drought is never due to one variable or a single event; rather, it occurs from a combination of factors, often working together to sustain dry conditions for days, months, or even years. With lack of rainfall leading to a gradual decrease in soil moisture, river flow, reservoir storage, and other factors (dependent on geographic area), the time when a drought is said to begin and end is unclear. This also makes the forecasting of drought initiation and termination difficult. More recently, the term "flash drought" has been used to describe the sudden onset of drought when meteorological conditions result in high temperatures and low soil moisture in a matter of weeks to a season (Senay et al. 2008). Studies of flash drought onset are now being conducted in river basins worldwide (Mozny et al. 2012; Senay et al. 2008).

Drought management is necessary to minimize consequences on the environmental, social, and economic sectors of an affected region. Environmentally, droughts stress aquatic life and terrestrial vegetation, often through the depletion of river flows and soil moisture. Socially, droughts increase the risk to public health, including a greater threat of wildfires and low flow water contamination, and the unequal distribution of impacts and relief. Economically, there are often direct losses to the food and agriculture industries when crops are stressed. Further, water suppliers must make supply

cuts to customers when reservoir levels decline, and governments need to pay for drought relief programs. Over the years, these consequences have led to single droughts causing over tens of billions of dollars in damages. Ryu et al. (2014) report that the Texas drought of 2011 resulted in the costliest drought in the state, with an estimated $7.6 billion dollars in economic losses. Therefore, water managers need to develop watershed management plans to define how to overcome these possible consequences. Use of forecast models (Hallack-Alegria and Watkins 2005; Sharma and Panu 2012; Tabari et al. 2013), modeled drought indicators (e.g., Heim 2002; Liang et al. 1994; McKee et al. 1993; Palmer 1965), economic analyses (Cai et al. 2015), and State and Federal mitigation plans (Wilhite 1997; Wilhite et al. 2000) are all current practices of water managers and researchers to aid in minimizing negative drought impacts.

1.2. Seasonal Drought Forecasting

Modeling techniques are often useful tools for water managers for decision-making purposes, especially when predicting and planning for drought impacts. Seasonal forecasting is one method of predicting droughts. Models can predict watershed changes in future seasons for the onset of imminent drought conditions.

A number of studies have utilized models to assess the effects of drought and climate anomalies on watersheds across the globe. Some of these models measure drought based off of Land Surface Models (LSMs), others incorporate General Circulation Models (GCMs), and yet others use drought indices. These different models have been used for simulating past or future drought conditions (e.g., Luo and Wood 2007; Ryu et al. 2014; Sheffield and Wood 2007; Shukla et al. 2011; Tabari et al. 2013),

and simulating streamflows in river basins with climate forecasts (Sinha and Sankarasubramanian 2013). For example, Shukla et al. (2011) utilized an LSM to develop a drought management system in the State of Washington, which utilized seasonal hindcasting to predict the occurrence and end of drought conditions of four historical droughts. They found using an LSM for seasonal forecasting (or hindcasting) is applicable for aggregated geographic areas, whereas drought indices are only applicable to coarse spatial resolutions for predefined national climate regions. Sheffield and Wood (2007) also compared the results from an LSM as compared to drought indices, and discovered the LSM gave more accurate predictions of actual drought conditions than the Palmer Drought Severity Index (PDSI) for cooler regions as well as for shorter time scales (i.e., seasons) for major droughts.

GCMs are also widely used in drought modeling studies, and have been previously used to predict water balance and economic changes from climate anomalies (Cai et al. 2015; Sheffield et al. 2009; Sheffield and Wood 2008). Specifically, Cai et al. (2015) utilized a GCM and RCM (Regional Climate Model) for the Republican River basin to create a decision-support framework for water managers, and coupled the forecasts with simulation-optimization model for economic profits and costs of implementing drought mitigation techniques. The study is a good example of pairing the use of a GCM with an economic-based decision support tool.

GCMs and LSMs can also be used for assessing seasonal streamflows in river basins, which can be useful for predicting effects of drought and/or climate change on river systems. GCMs were used in seasonal streamflow studies on the Nile River basin (Beyene et al. 2009), the Aidoghmoush River basin in Iran (Ashofteh et al. 2013), and the

Vermilion River basin in Illinois (Tavakoli and De Smedt 2012) for predicting changes in river systems over multiple climate scenarios. Sinha and Sankarasubramanian (2013) also utilized an LSM coupled with an atmospheric GCM to generate skillful monthly probabilistic forecasts of streamflow and soil moisture in the Apalachicola River basin in Florida. The study presented herein focuses on utilizing a physically-based LSM for modeling skillful probabilistic seasonal streamflows for the purpose of season-ahead drought forecasting.

1.3. Problem and Research Motivation

A severe hydrologic drought afflicted central Texas from 2008 through 2015. Preliminary data for 2014 reveal that this drought has caused the Lower Colorado River basin to experience its driest conditions on record, making this the worst drought in the basin's history from a water supply perspective (Lower Colorado River Authority (LCRA) 2015a). The drought, in addition to the typically high variability of precipitation and streamflow in the region, has stressed Texas water managers to appropriately allocate water to municipalities. One such water management authority is the Lower Colorado River Authority (LCRA) in Austin, Texas. The LCRA manages six reservoirs (collectively known as the Highland Lakes) along the Lower Colorado River, providing water to 1.1 million residents in central Texas, hydropower within 55 counties, water for rice farming, and freshwater flows into Matagorda Bay. The two main reservoirs the LCRA manages for water supply are Lake Buchanan and Lake Travis. Combined storage in these two reservoirs reached a near record low of 32 percent of total capacity on September 19, 2013. In order to secure water for high priority municipal and domestic

use, the LCRA curtailed water supply from the Highland Lakes to most interruptible customers (e.g. rice farmers) annually from 2012 through the first half of 2015. Despite flooding in May 2015, the LCRA was still affected by the drought at the time of this research, with the combined storage volume at 71 percent of total capacity as of October 14, 2015.

There are concerns that Texas may be entering a new climate "norm" (Heo et al. 2015; Smith 2015). Since 2008, the LCRA has observed six of the ten lowest inflows on record, with the lowest occurring in 2011, the third lowest in 2013, and the second lowest in 2014 (see Table 1.1). Following the floods of 2015, the river quickly returned to low-flow conditions. The LCRA will consider the drought in the Highland Lakes to be over when both Lakes Buchanan and Travis are filled to 100 percent of capacity. In order for the lakes to fill, dry soils must become saturated (or partially saturated) long enough to sustain substantial flows into the lakes.

Table 1.1. Highland Lake's 10 Lowest Annual Inflows (1940-2014)

Rank	Year Occurred	Annual Total Inflow (acre-feet)
1	2011	127,802
2	2014	207,626
3	2013	215,138
4	2008	284,462
5	2006	285,229
6	1963	392,589
7	2012	393,163
8	1983	433,312
9	1999	448,162
10	2009	499,732

The LCRA is interested in reevaluating operations, policies, and water management strategies due to increasing concerns of climate variability. Previously, the LCRA had not included climate forecasts within water management plans or operations due to large variation in seasonal and annual streamflows, as well as the absence of observable watershed variables (e.g. snowpack). However, with increasingly constrained operations, non-stationarity in climate, and the availability of advanced forecasting technologies, the LCRA is seeking to update its Water Management Plan with seasonal predictive forecasts to support decision making on how to best allocate water to its customers. The LCRA is interested in expanding a previously developed hydroclimatic forecast model.

1.4. Research Hypothesis and Objectives

The overall collaborative research project tests the hypothesis that seasonal forecasts using a physically-based hydrologic model for the Lower Colorado River basin will give the LCRA increased confidence in making water allocation decisions with longer lead times (for example, extending from one month to three- or six- month forecasts). The objective of the research presented herein is to diagnose the skill of seasonal inflow forecasts through the use of the Variable Infiltration Capacity (VIC) and river routing models. The development, calibration, verification, and analysis of these models as a physically-based watershed model for the LCRA is the primary scope of this thesis. This objective is to be met by incorporating statistical climate forecasts with physical watershed components (such as previously observed meteorological data, and soil moisture components); calibrating the model based on historical runoff estimates;

and running the model with (historical) forecast inputs to generate season-ahead hindcasts. These hindcasts are then compared to observed inflows.

This thesis presents the work of developing the physically-based watershed model for the LCRA and diagnosing the initial model forecasts. Following this introductory chapter, Chapter 2 describes the context for water management by the LCRA and the characteristics of the Lower Colorado River. Background on the VIC model is also presented. Chapter 3 describes the set-up of the VIC and routing models specific to the Lower Colorado River watershed, and Chapter 4 describes the calibration and verification procedure. Chapter 5 presents the results of the first sets of hindcasts generated by the VIC model and an assessment of these results. Finally, Chapter 6 presents the conclusions from this study as well as the future work to be completed in order to utilize the VIC model in the LCRA's decision making and operating procedures.

Chapter 2. Background

2.1. Lower Colorado River Authority

The Lower Colorado River Authority (LCRA) was formed through the LCRA Act, passed by the Texas Legislature in 1934, as a conservation and reclamation district to serve the surrounding counties of the Lower Colorado River (LCRA 2010). Today, the LCRA serves 80 counties in four markets:

1. *Water management,* which includes flood management, hydroelectric power, water quality, and the control and proper allocation of the waters within the Lower Colorado River watershed for urban and agricultural use;
2. *Electrical energy*, which provides communities with electrical power, transmission, and energy services;
3. *Conservation,* including conservation programs for water scarcity, agriculture, and ecological benefits; and
4. *Lands,* which includes managing parks and recreation.

Figure 2.1 outlines LCRA's water service area in central Texas. The LCRA manages water along the Lower Colorado River from the City of San Saba to the Gulf of Mexico. The watershed extent is approximately 18,300 square miles, with the water service management area extending to 22,447 square miles.

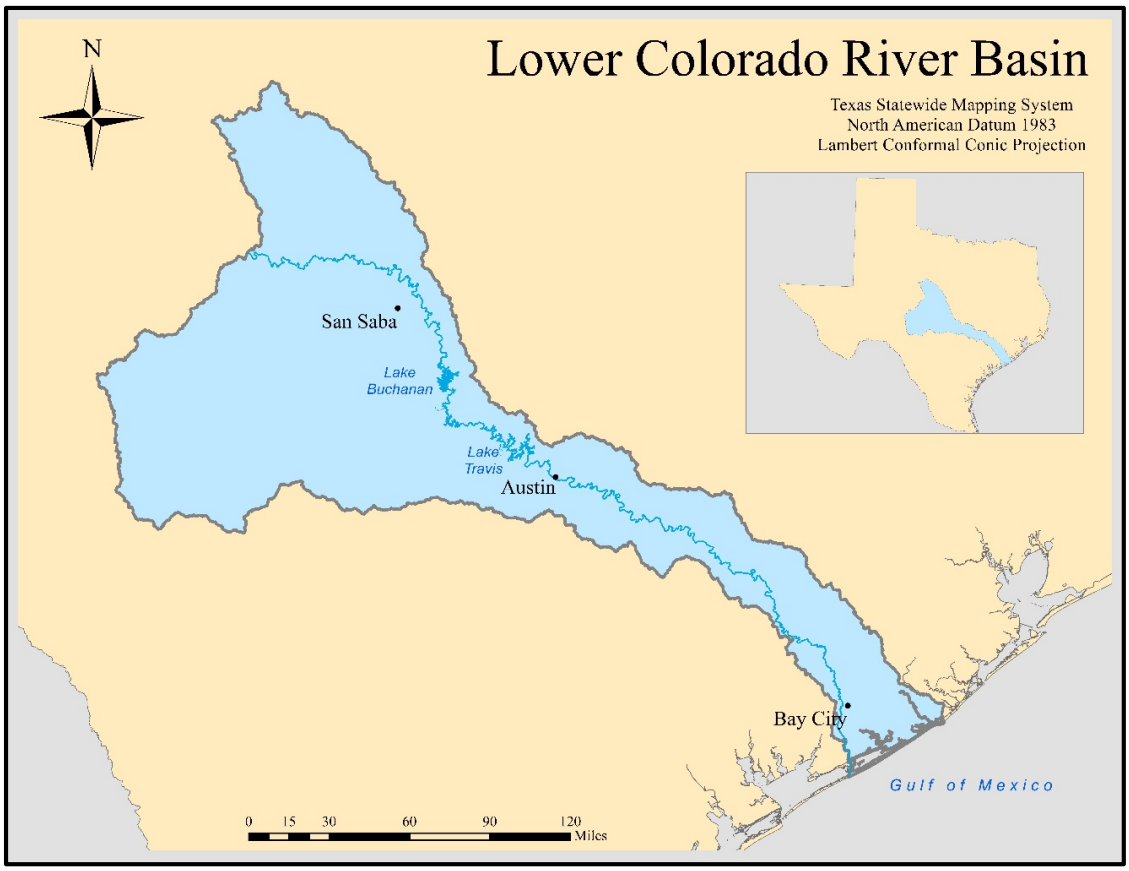

Figure 2.1. The Lower Colorado River Basin of Central Texas, managed by the LCRA. The watershed spans an area of 18,300 square miles. (Figure by author).

In order to manage flooding along the Colorado River, as well as manage water conservation in periods of drought, the LCRA developed a series of dams to form six lakes in the upper portion of the watershed known as the Highland Lakes system. Moving downstream, these lakes include Lake Buchanan, Inks, Lyndon B. Johnson (LBJ), Marble Falls, Travis, and Austin. Lakes Inks, LBJ, Marble Falls, and Austin are used for generating hydroelectric power and providing recreation, while Lakes Buchanan and Travis are the two primary reservoirs to collect and store water for water supply (LCRA 2015b). Since the four other lakes are kept at near constant levels for hydropower and

recreational purposes, only Lakes Buchanan and Travis are of interest for this study, with the research evaluating the change in water storage volumes in the reservoirs during times of drought.

Lake Buchanan is formed by Buchanan Dam. Construction of the dam began in 1931, and was completed in 1938. The dam is 145.5 feet high and 10,988 feet long, with a discharge capacity of 347,300 cubic feet per second (cfs) through the use of floodgates and turbines. The dam is used primarily for hydropower and water supply. Lake Buchanan can hold 875,588 acre-feet of water with a surface area of 22,017 acres when full (LCRA 2015c). Lake Travis is formed by Mansfield Dam, which was constructed between 1937 and 1942. The dam is 278 feet tall and 7,089 feet long, and has floodgates and turbines to supply a total discharge capacity of 133,400 cfs. Mansfield Dam was created for the primary purposes of water storage and supply, hydropower, and flood management. When at full capacity, the lake has a surface area of 19,297 acres and a volume of 1,134,956 acre-feet of water (LCRA 2015d).

Generally, the volumes of Lakes Buchanan and Travis are combined to represent the total available water supply. The two lakes can hold a total volume of 2,010,544 acre-feet of water. During the region's Drought of Record, which lasted between 1947 and 1957, the total water supply volume dropped to a record low of 621,221 acre-feet, equaling 31 percent of capacity, on September 9, 1952. In comparison, the drought beginning in 2008 dropped the water supply volume to the second lowest on record, at 637,123 acre-feet, or 32 percent of capacity, on September 19, 2013. Although the lakes never dropped further than the storage observed during the Drought of Record, the

drought beginning in 2008 is considered the worst hydrologic drought in history for the Lower Colorado River basin, as explained in section 1.3.

The LCRA allocates water from Lakes Buchanan and Travis via firm and interruptible water contracts. The LCRA has long-term, firm water contracts for municipal and industrial clients, and interruptible water contracts for agriculture. Firm water contracts are typically multi-year and guarantee municipalities, cities, and industries water rights and diversions in the case of a repetition of the Drought of Record. Interruptible water contracts, in contrast, are shorter contracts (about 1 year) with the agreement to allow the LCRA to interrupt or curtail the water supply as needed on a *pro rata* basis to protect the firm contracts during a repetition of the Drought of Record. If there is a period worse than the Drought of Record, then the LCRA will need to curtail water supply from firm customers, also on a *pro rata* basis, so that all firms will suffer equally during the drought period. The LCRA must also consider the competition of water demands between clients, maintain critical freshwater flows into Matagorda Bay to preserve ecological integrity, as well as adhere to the supremacy of the State of Texas regarding water resources allocation (LCRA 2010).

The LCRA adheres to its contracts and policies stipulated in its Water Management Plan. The Water Management Plan details the legal authority of the actions of the LCRA within the State of Texas, describes management policies for the interests of stakeholders, and details the actions of water conservation efforts and drought contingency plans to balance the multiple competing water demands on the Colorado River (LCRA 2010). The research conducted for this study includes the preliminary

testing of probabilistic drought forecasting techniques for potential incorporation in the LCRA's Water Management Plan.

2.2. Watershed Characteristics

There are seven basins which contribute flows into the Highland Lakes (see Figure 2.2). All flows from the Pecan Bayou basin and the Lake Buchanan basin contribute inflows into Lake Buchanan. These flows, along with flows from the Lake LBJ basin and the Lake Travis basin, all contribute to inflows into Lake Travis. The Pecan Bayou and Lake Buchanan basins have changed from former prairie land, and now the vegetation cover is dominated by shrub/scrub in this arid portion of the basin. The main land use in the Pecan Bayou basin is oil production, while the Lake Buchanan basin supports wheat agriculture in the Central Texas Plateau. South of these basins are the Lake LBJ basin and the Lake Travis basin, which drain into Lake Travis. Both of these basins lie in the Central Texas Plateau with a hilly savannah primarily used for cattle farming. Perennial streams flow into Lake Travis from these basins. The central portion of the Lower Colorado River watershed is unique, as urban sprawl has increased urbanized land cover near the City of Austin over many years. In the less urbanized areas, distinct grassland and prairie vegetation are present from the more humid climate and Blackland Prairie. The Lower and Matagorda basins contain pasture, hay, and cultivated crops for agriculture, as well as evergreen forests in the Texas hill country (LCRA 2006).

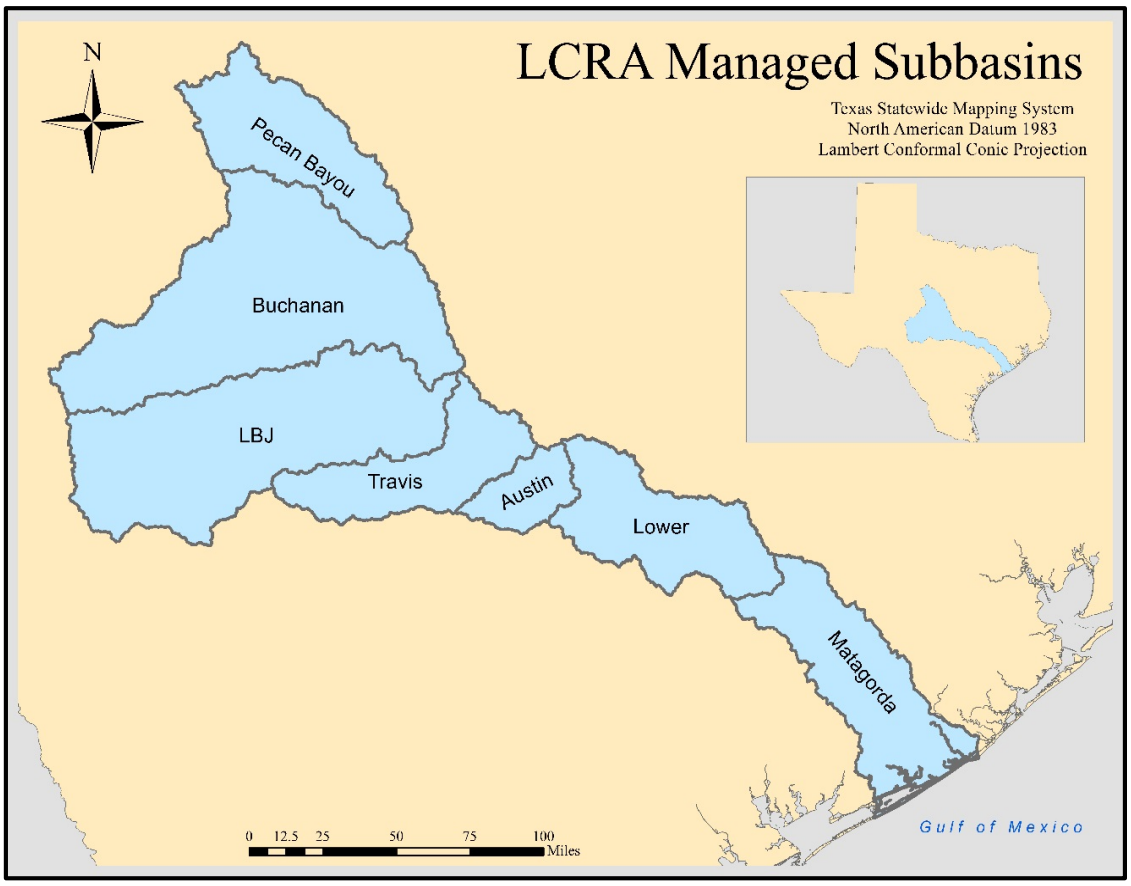

Figure 2.2. LCRA Managed Sub-basins in the Lower Colorado River Watershed. (Figure by author).

The Lower Colorado River basins consist of varying bedrock types. In the upper portion of the river basin (defined here as above Lake Travis), shale and mudstone dominate the Pecan Bayou and Lake Buchanan basins (Stoeser et al. 2005; United States Geological Survey (USGS) 2005). This northern area of the Lower Colorado River watershed also contains shallow, rocky soils with large granite and limestone outcrops and steep slopes (LCRA 2010). The Lake LBJ and Lake Travis basins consist of a mix of ambiphole schist, dolomite, granite, and sandstone in the central area, and limestone in the east (Stoeser et al. 2005; USGS 2005). Below Lake Travis, the Lower Colorado River

flows through shale and outcrop in the Texas hill country, until the bedrock changes at the Balcones Fault in Austin, Texas. Here, the soils change to that of sand, clay, and shale in the Blackland Prairie and coastal plains, where the watershed narrows as the river flows into Matagorda Bay (LCRA 2010). The large variability in soil consistency and depth across the basin largely influences the total volume of runoff and inflows into the reservoirs, especially from rainstorms over small areas. The deep, porous soils will easily lose soil moisture in times of little precipitation, making it hard to sustain river flows in tributaries to replenish the lakes during periods of drought.

The central Texas region has experienced five major droughts since 1947 until 2015. Central Texas droughts are often influenced by the varying climates the region experiences. The Lower Colorado River watershed is arid in the far western portions of the State and humid near the Gulf of Mexico. The annual precipitation follows a general trend of increasing from the west to the east. From precipitation data collected between 1981 through 2010 and compiled using the Parameter-elevation Relationships on Independent Slopes Model (PRISM: Daly et al. 2008; Daly et al. 1994), the average annual precipitation is 21 inches per year in the far western portion of the watershed. Near the Gulf, this number increases up to 52 inches per year. This increase is partly because the region receives more moisture from the tropics, and also because tropical storms and hurricanes, which make landfall off of the coast of the Gulf of Mexico, can increase precipitation amounts significantly. In the Highland Lakes system, Lakes Travis and Buchanan are located within the Texas Hill Country. Lake Travis receives about 30 to 31 inches of precipitation per year, whereas Lake Buchanan receives about 28 to 29 inches per year. Due to the geographic location of Texas, the watershed does not receive

much snow. Therefore, snow accumulation and snow melt are not key components in the water budget for the watershed, and are typically not included in Texas watershed models. Despite these average precipitation values listed above, precipitation is extremely variable within central Texas. The mixing of arid and humid climates can produce severe storms over small geographic areas, resulting in large amounts of precipitation and high flows observed in a small portion of the watershed. Soils can also dry quickly, and streamflows recede during hot, dry summers.

2.3. Ensemble Streamflow Prediction

Ensemble Streamflow Prediction (ESP) is a forecasting procedure to generate probabilistic streamflow forecasts. The procedure was developed for prediction of short-term and seasonal streamflows based on climate data and watershed characteristics using statistical evaluations (Day 1985; Smith et al. 1992; Twedt et al. 1977; Wood and Schaake 2008). The procedure utilizes hydrologic and hydraulic models with variables representing the watershed's conditions at the time of forecast, including (recent) precipitation, evaporation, soil moisture, snow, and observed streamflow, among others. ESP forecasting also presumes past observed meteorological conditions present possible future meteorological conditions. The hydrologic or hydraulic model utilizing ESP assesses these watershed conditions to statistically generate a time-series of probabilistic forecasts of streamflow for the specified time-series window for a given time step. The ESP procedure can also be applied to generate "hindcasts," based on historical meteorology and observed watershed conditions, to verify the model's accuracy; if there are no biases or errors in the models, then streamflow variables produced by the ESP

hindcasts should match the historically observed conditions for the watershed (Day 1985). Figure 2.3 describes the overall process of ESP.

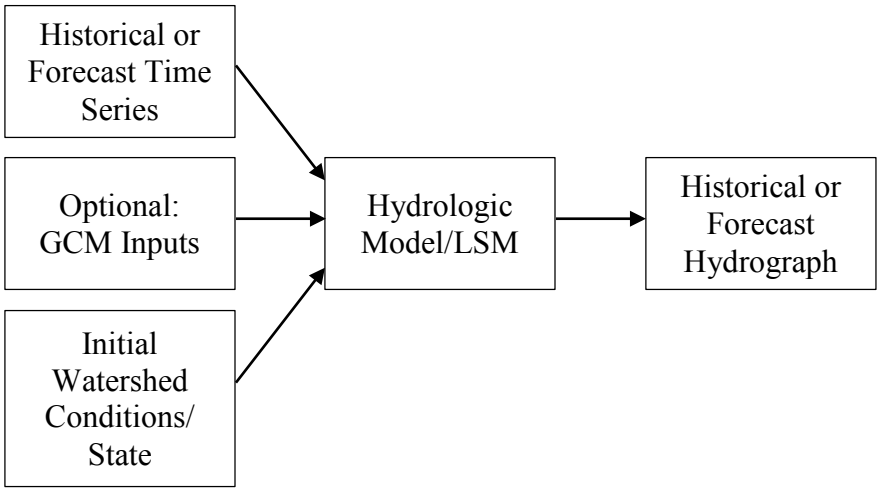

Figure 2.3. Procedure of ESP in Hydrologic Modeling. Adapted from Figure 3 in Day (1985).

Utilizing ESP can be an important tool in streamflow forecasting methods and reservoir management. Hamlet and Lettenmaier (1999) used ESP along with six climate models simulating ENSO and PDO effects on the Columbia River Basin in the Pacific Northwest. Results discovered linkages between climate patterns and annual flow patterns to generate skillful forecasts, which can be used for appropriate reservoir management for when streamflows are likely high versus low due to climate patterns. Faber and Stedinger (2001) incorporated ESP in Sampling Stochastic Dynamic Programming (SSDP) for the purposes of optimized reservoir management. The ESP was found to estimate appropriate seasonal inflows as well as incorporate the most current watershed conditions when assessing reservoir management operations. Specifically

related to drought, managers can analyze the predictions of critically low streamflows in river and reservoir systems to determine if contingency measures or actions need to be implemented (Day 1985).

2.4. Variable Infiltration Capacity (VIC) and Routing Models

The Variable Infiltration Capacity (VIC) model is a macroscale hydrologic model which spatially simulates water and energy balances over a gridded land surface (Liang et al. 1994). The model incorporates soil and vegetation heterogeneity in the land surface using a soil-vegetation-atmosphere transfer scheme, or SVATS. VIC can either be coupled with a GCM to generate long-term forecasts or hydrologic projections, or it can be coupled with a numerical weather prediction (NWP) model to generate short-term hydrologic forecasts (Liang et al. 1994). Using meteorological forcings from GCMs or NWP models (e.g., precipitation, temperature, wind speed) and physical watershed components (e.g., soils, land cover, topography), VIC calculates water and energy fluxes at a designated time step for each grid cell. Specific details on VIC methodology and calculations are described in Liang et al. (1994). The primary water balance processes computed in VIC are displayed in Figure 2.4.

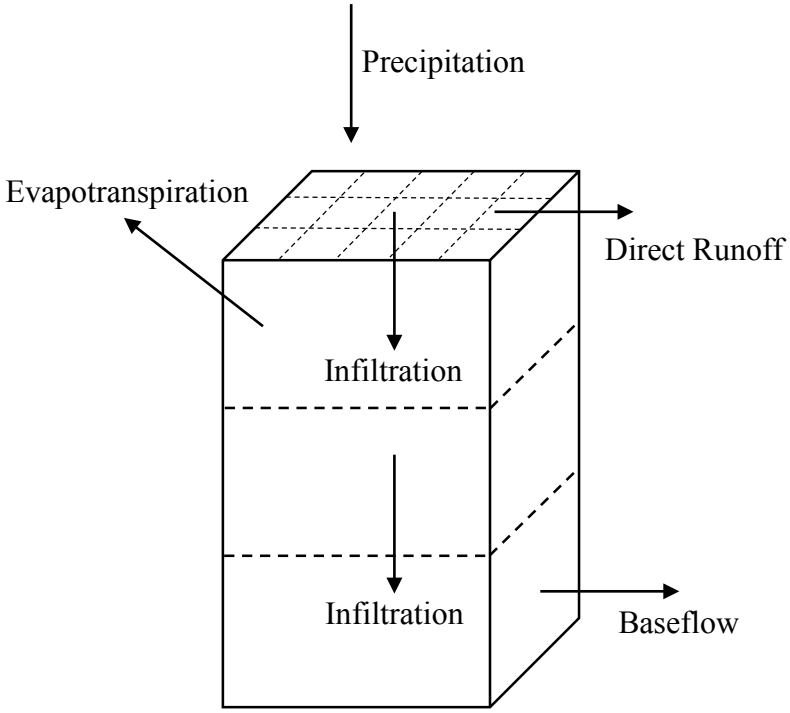

Figure 2.4. VIC Water Balance Representation with Three Soil Layers.

VIC couples with a separate routing model, which takes the generated VIC fluxes for each grid cell and routes the predicted runoff through the watershed of interest. The model routes runoff through each grid cell to accumulate runoff through the grid network. This accumulation calculates an impulse response function (unit hydrograph) for the basin. The impulse response function relates increased river flows to direct runoff in the watershed as attributed from VIC water balance output (Lohmann et al. 1996). In order to route the runoff and baseflow, the model solves the linearized Saint Venant equation while maintaining continuity.

VIC is a versatile hydrologic model which has been used in multiple studies as an LSM or utilizing a GCM. Utilizing VIC output to predict streamflow, Lohmann et al. (1998b) and Nijssen et al. (1997) validated results generated from the routing model with that of observed streamflow. Lohmann et al. (1998b) accurately predicted runoff to the Weser River in Germany, but also discovered knowledge of the relationships between the VIC input parameters is needed when applying VIC and the routing model to ungauged basins. Nijssen et al. (1997) also accurately measured streamflow in the Delaware and Columbia Rivers in the Northeast United States, but found results are also dependent on infiltration and subsurface processes. Other studies have used VIC to address physical watershed components and water budgets under changing climates (Abdulla et al. 1996; Andreadis and Lettenmaier 2006; Beyene et al. 2009; Stamm et al. 1994), as well as for generating seasonal streamflow forecasts in river basins (Acharya et al. 2012; Hamlet and Lettenmaier 1999; Qiao et al. 2014; Wood and Lettenmaier 2006; Wood and Schaake 2008). VIC has also been used specifically for predicting drought conditions. VIC was utilized in the drought studies conducted by Luo and Wood (2007), Ryu et al. (2014), Sheffield and Wood (2007), and Shukla et al. (2011), which are described in Chapter 1.

More information regarding VIC and the routing model can be found at http://vic.readthedocs.org/en/master/.VIC and the routing model are open source, and the most updated versions are available for download at https://github.com/UW-Hydro/VIC. A description of how to run VIC and the routing model is provided in Appendix A.

2.5. Previous Work for the LCRA

Previously, the LCRA's water management has included more deterministic rather than probabilistic analyses. To help aid the LCRA in probabilistic estimations and better manage firm and interruptible water supply contracts, Watkins et al. (2000) developed a stochastic optimization model to maximize revenues in water supply contracts and recreation in periods of streamflow uncertainty or drought. Kracman et al. (2006) further expanded this model to include maximization of revenues in the agriculture and hydropower sectors. The LCRA is seeking to incorporate climate and streamflow forecasts with management decisions. Due to high streamflow variability in central Texas, more recent models have been developed for the LCRA to incorporate probabilistic streamflow forecasting into their water management strategies. Wei and Watkins (2011) generated probabilistic streamflow forecasts through the use of a seasonal statistical forecast model incorporating climatic and oceanic processes.

In another study, CH2M HILL was contracted to create a model to evaluate future climate change impacts. CH2M HILL utilized VIC to provide a way to physically model the basin response with eight climate scenarios from GCMs. The model developed by CH2M HILL predicts long range inflows; results indicate inflows to Lake Travis are likely to decrease through 2050, and will continue to decrease through 2080 (CH2M HILL 2008).

The research in this thesis extends the VIC model produced by CH2M HILL (2008), which used VIC version 4.0.7, for seasonal, short-term probabilistic streamflow forecasting using a physically-based watershed modeling approach. As compared to the previous statistical models developed for the LCRA, VIC is beneficial in that it can

account for spatial variability of rainfall across the watershed, it can assimilate soil moisture through its variable infiltration curve and water balance calculations, and it can be updated for changes in land use and land cover conditions.

Chapter 3. Model Set Up

3.1. VIC and Routing Model Input Files

Many input files to VIC and the routing model were adjusted appropriately to make the model physically-based to the Lower Colorado River basin. VIC version 4.1.2.k was used in this study (updated from version 4.0.7), as it was the most updated version of the model available at the start of this study. The VIC model uses a global parameter file to describe overall model parameters and methods, and to define the names and directories of all necessary data inputs. To define the physical characteristics of the watershed, single files representing a soil, a vegetation, and snow (elevation) bands are used as inputs, with each grid cell of the model consisting of a separate line in the file. To incorporate meteorological data, VIC reads in individual meteorological forcing files for each grid cell. These meteorological forcing files give meteorological data on a daily time step, and is the only input using a time dimension. Although VIC is capable, snow balances are not incorporated into the LCRA's analysis due to negligible snow amounts in the region; however, a snow bands input file is included to represent the land surface elevation. Also, water storage balances of lakes are not incorporated because only the unregulated monthly inflows into Lakes Buchanan and Travis are of interest.

VIC analyzes all input parameters and data to simulate the components of a water and energy balance; these fluxes are written to output flux files, which are then fed into the routing model. Although different versions of the routing model have been developed outside of the University of Washington, Rout1.0 (Lohmann et al. 1996) is the only validated version of the routing model, and therefore is the version being implemented in

this study. The current versions of VIC and the routing model are posted at http://vic.readthedocs.org/en/master/Development/CurrentVersion/.

Routing model input files represent the flow routing network across the gridded basin; a fraction file and flow direction file assign specific values for each grid cell, while in this study the flow velocity, flow diffusion, and xmask parameters are assumed constant across the watershed. These constant values are used to create unit hydrographs routed to each station, which can be used as inputs in future routing models (called uh_s files). The VIC and routing model inputs are based on those from the climate change study conducted by CH2M HILL (2008), and were updated to appropriately model the Lower Colorado River basin using physically-based, observed datasets in streamflow forecasting.

Descriptions of each input file for the VIC model and routing model are presented in Tables 3.1 and 3.2, respectively. All input files required to run the model are provided in the "01Model" folder in the supplemental materials.

Table 3.1. VIC Model Input Files

Name	Description	Format	Database
Global Parameter File	Describes the hydrologic methods and names/directories of other input files.	Text File	Prepared by user.
Meteorological Forcing Files	Historical time series of precipitation (mm/d), maximum temperature (°C), minimum temperature (°C), and wind speed (m/s). Each grid cell is provided a full time series.	American Standard Code for Information Interchange (ASCII) File	Livneh et al. (2013)
Snow Bands/Elevation Parameter File	Defines snow (elevation) bands per grid cell for separate simulation, instead of modeling grid cells as flat terrain. A value of 6 snow bands is defined per grid cell.	ASCII File	North American Land Data Assimilation System (NLDAS) (Mitchell 2004)
Soil Parameter File	Defines an identification number, geographic information, and soil moisture conditions for each grid cell.	ASCII File	State Soil Geographic (STATSGO) database (United States Deapartment of Agriculture (USDA) 1991)
Initial State File	Describes the calculated soil moisture, water and energy conditions of the watershed state at a specific time period during a VIC simulation.	ASCII File	Output by VIC (optional)
Vegetation Library File*	Describes land cover and vegetation types.	ASCII File	NLDAS
Vegetation Parameter File	Describes number of vegetation types and fractional areas covering each grid cell.	ASCII File	NLDAS

*Files were unmodified from CH2M HILL (2008) model.

Table 3.2. Routing Model Input Files

Name	Description	Format	Database
Fraction File	Describes the fraction of each grid cell which produces runoff into the basin.	ASCII File	Prepared by user.
Flow Direction File	Assigns a flow direction value for each grid cell creating the flow network through the basin.	ASCII File	Prepared by user.
Flow Velocity File*	Describes the velocity parameter for river routing calculations per grid cell.	ASCII File	A constant value of 2 (m/s) is used.
Flow Diffusion File*	Describes the flow diffusion parameter for river routing calculations per grid cell.	ASCII File	A constant value of 800 (m^2/s) is used.
Xmask File*	Describes the size of the grid cell.	ASCII File	A constant value of 12,500 (m) is used.
Station Location File	Describes to which stations in the basin to route flows.	ASCII File	Prepared by user.
UH File*	Describes the grid impulse response function (unit hydrograph).	ASCII File	Prepared by user.
Runoff Time Series Files	Flux files outputted from VIC describing water and energy balances.	ASCII File	Prepared by VIC.
uh_s File (optional)	Describes routed flows to each station based on watershed velocity and flow diffusion.	ASCII File	Output by Rout1.0

*Files were unmodified from CH2M HILL (2008) model.

3.2. Data Compilation and Processing

3.2.1. Data Collection

Meteorological forcings data used are from the gridded meteorological dataset of the South Central (Gulf) basin compiled by Maurer et al. (2002). This dataset represents watershed states and fluxes for the conterminous United States from 1949 through 2000

(later extended to 2010) at a 1/8° scale. These data have been used extensively in hydroclimatic models, including hydrologic simulations of watershed state and energy balances and drought predictions (Andreadis and Lettenmaier 2006; Sheffield et al. 2004a). This dataset, prepared by Maurer et al. (2002), includes daily precipitation and temperature data taken from Cooperative Observer (Co-op) stations belonging to the National Climatic Data Center (NCDC), which were processed on a gridded basis using the synergraphic mapping system (SYMAP) algorithm (Shepard 1984). Then, Maurer et al. (2002) scaled the precipitation according to PRISM (Daly et al. 1994; Daly et al. 1997) for a 1961 to 1990 climate model. Wind speed was processed using linear interpolation from the National Centers for Environmental Prediction/National Center for Atmospheric Research (NCEP/NCAR) reanalysis on an approximately 1.9°-sized grid (Kalnay et al. 1996). Then, Livneh et al. (2013) expanded the meteorological forcings dataset by Maurer et al. (2002) to range from 1915 through 2011 at a finer spatial resolution of a 1/16° grid. Livneh et al. (2013) processed the updated forcings using the same techniques as Maurer et al. (2002). Specifics in slight processing modifications for certain components are explained in detail in Livneh et al. (2013). Because the meteorological dataset developed by Livneh et al. (2013) is an updated version of the dataset developed by Maurer et al. (2002), and includes a longer period of record, the forcings dataset by Livneh et al. (2013) was chosen for this study. The files are processed as ASCII files and aggregated to a 1/8° resolution. This process is described in Appendix B. These forcings are publically available for download from the U.S. Bureau of Reclamation at ftp://gdo-dcp.ucllnl.org/pub/dcp/archive/OBS/livneh2014.1_16deg/.

The meteorological forcings to be used by VIC to generate seasonal forecasts are generated using a forecast model developed at the University of Wisconsin Madison. More details in regards to their formation specific to this study are described in section 5.1.

3.2.2. Soil Depth Processing

In order to better represent spatial variability in soil characteristics across the Lower Colorado River basin, and to improve initial model performance (section 4.1), the State Soil Geographic (STATSGO) database was chosen to model soil depth. This database describes the soil texture for multiple soil layers across the conterminous United States at a 1:125,000 scale (USDA 1991). The finer resolution Soil Survey Geographic (SSURGO) data from the National Cooperative Soil Survey were also considered for use, but a large portion of data in the southern portion of the Lower Colorado River basin was not available. The STATSGO database, though a broader scale than SSURGO, was deemed appropriate for physically modeling the 18,300 square mile size of the Lower Colorado River basin. Data from the STATSGO database were collected from the Soil Information for Environmental Modeling and Ecosystem Management download center at Pennsylvania State University's Center for Soil Informatics (Pennsylvania State University 1998).

VIC represents the soil depth of each grid cell as three separate layers. Analysis of the NLDAS dataset for soil depth used in the CH2M HILL (2008) study revealed soil depth in each layer across the watershed did not vary much spatially. In the NLDAS dataset, the first soil layer ranges from 0.1 to 0.2 meters thickness; the second soil layer

ranges from 0.3 to 0.5 meters thickness, and the third soil layer is consistently 1 meter thick for all grid cells. This lack of variability in terms of total soil depth variability is revealed in Figure 3.1.

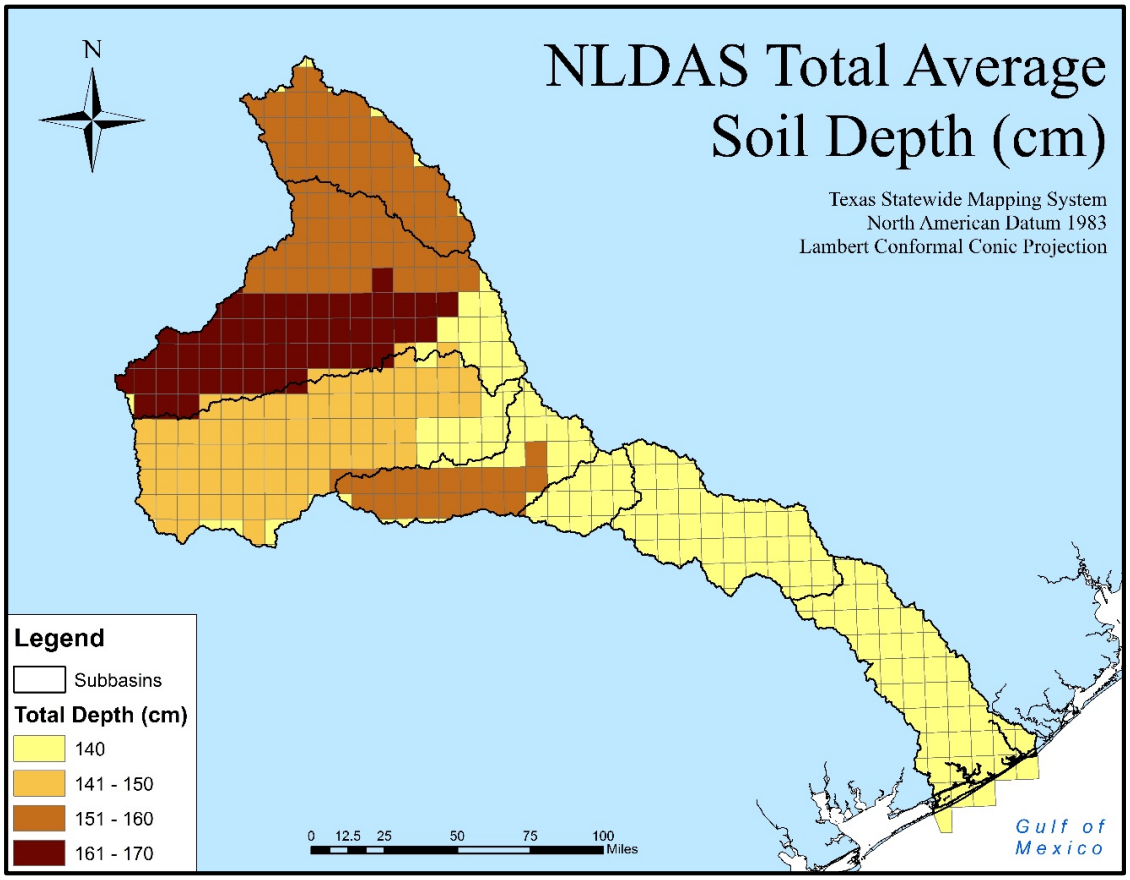

Figure 3.1. Total Average Soil Depth of the Lower Colorado River Basin using the NLDAS Database. (Figure by author).

In order to allow for spatial variability of soil thickness and layers across the watershed, the soil depths from STATSGO were compared. STATSGO is set up on a hierarchical scale where an identification code identifies separate soil polygons, called map units. The identification code for each map unit (MUID) is related to multiple sequence numbers which refer to the distribution of soil types and associated soil layers

across the map unit. The depth of each soil layer, as well as the soil textures, are then referenced by sequence number (USDA 1991). Soil layers ranged between three and six layers. Because the VIC soil input file is limited to three soil layers, the STATSGO data were processed into three soil layers using spatial averaging methods. First, sequence numbers with more than three soil layers were combined into three layers based on texture. Then, the average soil depths of these three layers were computed by taking the difference in the high and low soil depth elevation over the number of different unique sequence numbers. Soil layer breaks were reevaluated so that the depth of the first soil layer is never greater than the depth of the second soil layer, as required for VIC to run properly. The detailed procedure explaining how all identification numbers were separated into three soil layers is listed in Appendix C. Since the average depth of each soil layer was calculated per sequence number in each map unit, map units were intersected on the 1/8° grid extent of the Lower Colorado River basin in order to compute spatially weighted averages of soil depth for each layer per grid cell.

Figure 3.2 shows the results of the STATSGO total soil layer depth variability across the Lower Colorado River watershed. Comparing this map to Figure 3.1, it is evident that the STATSGO dataset represents more spatial variability in soils across the basin than does the NLDAS dataset.

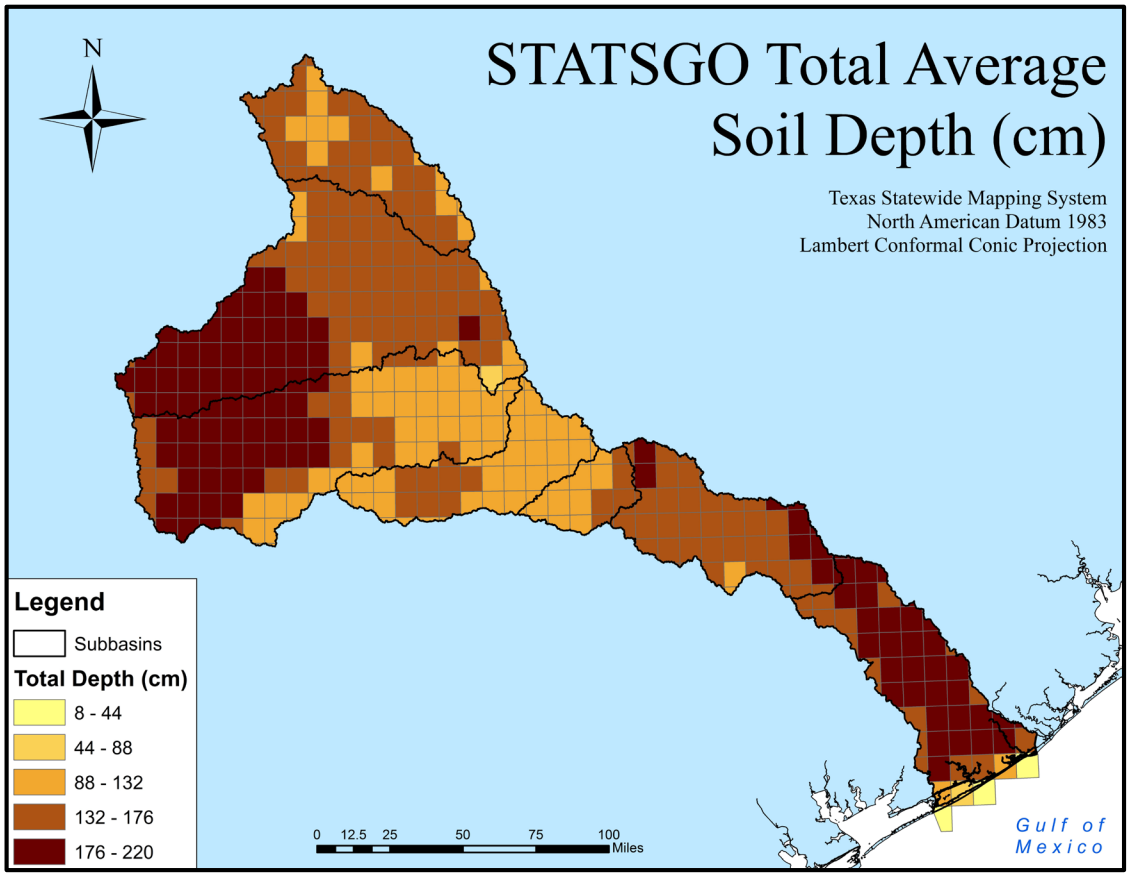

Figure 3.2. Total Average Soil Depth in the Lower Colorado River Basin using the STATSGO Database. (Figure by author).

3.2.3. VIC Model Set Up

The VIC model has multiple options for computing water and energy balances, which are defined in the global parameter file. The methods are unchanged from the CH2M HILL (2008) study: the ARNO method (Franchini and Pacciani 1991) is chosen for computing baseflow in the water balance, and calculations of frozen soils, snow analyses, turbulent fluxes, and lake simulations are disabled.

To analyze the Lower Colorado River basin on a 1/8° spatial resolution, Geographic Information System (GIS) attribute data were used to determine which grid cell coordinates encompass the lower basin extent. A 1/8° grid of Texas was overlain on the Hydrologic Unit Code 8 (HUC 8) watersheds of the basin using ESRI® ArcMap GIS software. Clipping around O.H. Ivie reservoir (managed independently by the Upper Colorado River Authority), the HUC 8 sub-basins included in the Lower Colorado River extent include Austin/Travis Lakes, Brady, Buchanan/LBJ, East Matagorda Bay, Jim Ned, Llano, Lower Colorado, Lower Colorado/Cummins, Middle Colorado, North Llano, Pecan Bayou, Pedernales, San Bernard, San Saba, and South Llano sub-basins. Placing the grid on these sub-basins resulted in a total of 399 grid cells encompassing the Lower Colorado River basin, of which 397 have associated meteorological forcings in the South Central (Gulf) region. The two missing files are for two grid cells located on the western border of the Lower Colorado River basin. The area of the watershed these cells contribute is less than 4.061 km^2 area, and therefore this small area does not have a large impact on the river flows and were left out of this study. A map of the grid cell coordinates of the Lower Colorado River basin is given in Appendix D.

The soil parameter file, vegetation parameter file, and snow band/elevation parameter file from CH2M HILL (2008) included grid cells in the upper basin of the Colorado River watershed, above O.H. Ivie reservoir. Since water flow into O.H. Ivie reservoir is consumed in the Upper Colorado River basin, it is assumed all area above this reservoir is noncontributing to the Lower Colorado River basin managed by the LCRA. Therefore, the soil parameter file, vegetation parameter file, and snow band/elevation parameter file were edited to only contain the grid cells in the Lower Colorado River

basin extent portrayed in Figure 2.1. This was done through bash shell LINUX programs listing the 397 grid cells of the lower basin and extracting the related data for these cells from the original file. All of the LINUX scripts used in this process are included in the "02External_Scripts" folder in the supplemental materials.

3.2.4. Routing Model Set Up

Adjustments to the routing model consisted of editing the input files to route flows only to the Lake Buchanan and Lake Travis stations (CRBU and CRTR, respectively) in the Lower Colorado River basin. Since the flow direction file and fraction file from the CH2M HILL (2008) study incorporated data for the grid cells of the upper portion of the basin, the fraction and flow direction files were revised to represent only the lower basin in the routing procedure for this study. The flow direction determines which grid cells are routed to each station. Flow direction is a raster input, based on the numerical scheme as depicted in Figure 3.3.

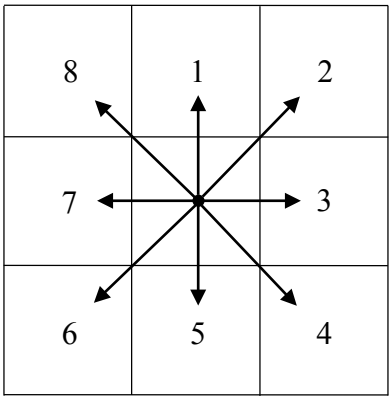

Figure 3.3. Flow Direction Scheme. The numeric designation determines the direction the flow will be routed from a cell.

If the middle square is the cell of interest to be routed, then that cell is assigned a value from 1 through 8, corresponding to the directions as shown in the grid. For instance, if the cell is labelled with the number 1, then the flow is to be routed to the cell directly north; if 2, then the flow is to be routed to the northeast; if 3, then the flow is to be routed to the east, and so on. For any grid cell that borders the lower basin boundary but is outside of the basin, the flow direction was changed to route flows away from the basin. It was verified that no grid cells outside of the basin would route extra flows into the basin. For those grid cells in the upper basin (above O.H. Ivie reservoir), a flow direction value of -1 was assigned to represent a "NO DATA" value.

The input file representing the fractional area of each grid cell was also revised to ensure the proper area is routed through the lower basin. In the original file from CH2M HILL (2008), there was a "NO DATA" value assigned as -9999. However, when this was run through the routing model, this NO DATA value was read as a contributing fractional value and would miscalculate the routed flows. Therefore, all "NO DATA" values were changed to -1 outside of the basin boundary, and any grid cell with noncontributing flow within the lower basin was assigned a value of 0.

After the flow direction and fraction files were adjusted to appropriately route flows through the lower basin, the stations file was adjusted to include only station locations for CRBU and CRTR, in order to only route flows through the Lake Buchanan and Lake Travis basins, respectively. The updates provided to the flow direction and station files resulted in 118 active grid cells which route to CRBU and 223 active grid cells which route to CRTR, meaning there are 105 cells downstream of the CRBU basin

which route into CRTR. The characteristics of these two basins were used to calibrate the VIC model, as described in Chapter 4.

Chapter 4. Calibration and Verification

4.1. Evaluating Model Performance

The VIC model performance was assessed using several statistics, including Pearson correlation (r) and coefficient of determination (r^2), Nash-Sutcliffe Efficiency (NSE), and the percent bias. These statistics were calculated to evaluate the initial VIC model (CH2M HILL 2008) during both the calibration/verification stage and for the hindcasting results presented in Chapter 5.

The Pearson correlation coefficient (r) measures the association of two data sets assuming a linear relationship. The Pearson coefficient of determination (r^2) is simply the square of the correlation coefficient, providing the same measure. The Pearson correlation coefficient is calculated as:

$$r = \frac{\sum_{i=1}^{n}\left(Q_{0,i} - \overline{Q_0}\right)\left(Q_{pred,i} - \overline{Q_{pred}}\right)}{\sqrt{\sum_{i=1}^{n}\left(Q_{0,i} - \overline{Q_0}\right)^2 \sum_{i=1}^{n}\left(Q_{pred,i} - \overline{Q_{pred}}\right)^2}} \quad (4.1)$$

where n = the total number of forecast streamflow observation pairs, $Q_{0,i}$ is the observed streamflow in time period i, $\overline{Q_0}$ is the mean of the observed streamflow, $Q_{pred,i}$ is the predicted streamflow in time period i, and $\overline{Q_{pred}}$ is the mean of the predicted streamflow.

The Nash-Sutcliffe efficiency (NSE) is based on the ratio of the sum of squared errors of the predicted streamflow to the variance in the observed streamflow. In the case where the NSE is less than zero, the average streamflow would be a better predictor than the modeled streamflow. Using the same notation as above, NSE is calculated as:

$$\text{NSE} = 1 - \frac{\sum_{i=1}^{n}\left(Q_{0,i} - \overline{Q_0}\right)^2}{\sum_{i=1}^{n}\left(Q_{0,i} - \overline{Q_{pred}}\right)^2} \quad (4.2)$$

Lastly, the percent bias is calculated as the difference between the predicted and observed streamflow according to the formula:

$$\text{Bias (\%)} = \frac{\sum Q_{pred,i} - \sum Q_{0,i}}{\sum Q_{0,i}} * 100 \quad (4.3)$$

To evaluate initial model performance, the model obtained from LCRA (CH2M HILL 2008) was run using the clipped watershed extent (representing only the sub-basins contributing to Lakes Buchanan and Travis) on the original NLDAS soil and vegetation input files and parameters. The performance statistics are calculated for the total unregulated inflows into both lakes, as presented in Table 4.1.

The low NSE values and large (negative) bias in Table 4.1 reflect consistently low flow predictions through the time period relative to the historically unregulated, observed flows documented by the LCRA. Also, it is noted that there are lower correlations during the periods of 1940 through 1960. The NLDAS vegetation file uses the University of Maryland's vegetation classification, modeling vegetative cover from 1981 to 1994 (NASA 2015a). It is possible that the model poorly simulates prior years due to changing land cover.

Table 4.1. VIC Model Performance by Decade: Initial Model with NLDAS Soil File

Decade	r^2	r	NSE	Bias (%)
1940	0.391	0.625	-0.278	-73.6
1950	0.379	0.616	0.182	-71.1
1960	0.671	0.819	0.029	-69.4
1970	0.493	0.702	0.132	-67.5
1980	0.680	0.825	0.134	-65.8
1990	0.692	0.832	0.359	-64.9
2000-2011	0.779	0.882	0.381	-60.4
1940-2011	0.534	0.731	0.201	-67.5

The soil parameter file was updated using the STATSGO database (as detailed in section 3.2.2), and a new run of the initial model was performed, with results given in Table 4.2.

Table 4.2. VIC Model Performance by Decade: Initial Model with STATSGO Soil File

Decade	r^2	r	NSE	Bias (%)
1940	0.335	0.578	0.263	-27.1
1950	0.621	0.788	0.603	-41.8
1960	0.638	0.799	0.628	-0.325
1970	0.759	0.871	0.714	11.8
1980	0.778	0.882	0.708	13.4
1990	0.828	0.910	0.795	5.05
2000-2011	0.757	0.870	0.666	62.9
1940-2011	0.679	0.824	0.654	-0.758

4.2. Calibration Parameters

There are many parameters used within the VIC and routing models, but a small set of parameters are recommended for calibration. This is because the spatial variability

of some parameters cannot be well represented using satellite or geological observations, and others are not physically-based but are just used in mathematical operations to define the soil infiltration capacity curve (University of Washington 2015). Further, determining which parameters to calibrate depends on the particular study; parameters can be calibrated according to soil, snow, or canopy calculations. Since central Texas receives minimal snow and does not have large canopy vegetation, the VIC model in this study is calibrated by optimizing soil parameters. The main soil parameters which have the greatest influence on the hydrograph, and therefore are suggested for calibration (Gao et al. 2010; Liang et al. 1994; Nijssen et al. 1997), are as follows:

1. b_{infilt}: describes the available infiltration capacity over the grid cell. This parameter defines the shape of the Variable Infiltration Capacity curve.
2. *Ds*: represents the fraction of Ds_{max} where non-linear baseflow is observed.
3. Ds_{max} (mm/d): represents the maximum baseflow from the bottommost soil layer in the model.
4. *Ws*: represents the maximum soil moisture fraction where non-linear baseflow is observed in the bottommost soil layer in the model.
5. Soil Depth (m) (all three layers): represents the thickness of three soil layers. With thicker soil layers, more water is stored within the soil matrix and is available for evapotranspiration.

The parameters b_{infilt} and *Ws* define shapes of mathematical curves in the model, whereas *Ds*, Ds_{max}, and soil depth are based on physical watershed characteristics. *Ds* and Ds_{max} are adjusted according to soil characteristics such as soil moisture and saturated

hydraulic conductivity, and soil depth is adjusted according to spatial variability of soil layers across the watershed (Gao et al. 2010; Liang et al. 1994).

There are also many parameters in the routing model which could be calibrated, but for studies on a monthly time scale, calibration of the routing model is generally not necessary (University of Washington 2015). Some routing inputs, such as flow direction and fractional contribution of runoff from each grid cell, can be obtained from GIS analysis using a Digital Elevation Model (DEM); other physical parameters such as velocity or flow diffusion can be measured *in situ*, but also can be set to typical values when modeling on a monthly or larger time step (University of Washington 2015). Calibration for analyses on shorter than a monthly time scale is described in Lohmann et al. (1996), Lohmann et al. (1998a), and Lohmann et al. (1998b).

4.3. Sensitivity-based Radio Tuning Calibration Tool

Calibration of the initial VIC model was completed in order to match the simulated streamflow to the observed streamflow, as estimated by LCRA. Studies have calibrated the VIC model using the Multi-Objective Complex Evolution (MOCOM-UA) method (Yapo et al. 1998) and the multisite cascading calibration (MSCC) method (Xue et al. 2015). Calibration for the LCRA study was done by adjusting the seven parameters described above through a Sensitivity-based Radio Tuning Calibration tool (SRTC) (CHI Support 2015). This tool, which was adapted from the hydrologic modeling program PCSWMM (PC Stormwater Management Model) for use in this study, allows the manipulation of model parameters according to a user-defined percentage change. This change, either a percent increase or a percent decrease from the original value, is bounded

according to user-defined upper and lower bounds for each parameter. When a parameter is adjusted, the SRTC linearly interpolates between simulation results based on the parameter's extreme value according to the equation:

$$Y_{calib} = \sum_{i} \left(\max(W_i, 0) * \left(Y_{i,max} - Y_{init} \right) + \min(W_i, 0) * \left(Y_{init} - Y_{i,min} \right) \right) \quad (4.4)$$

where Y_{calib} is the new calibrated streamflow value, i is the parameter of interest to be calibrated, W_i is the weighted scale value ranging from -1 to 1 for parameter i, $Y_{i,max}$ is the maximum value of parameter i, $Y_{i,min}$ is the minimum value of parameter i, and Y_{init} is the initial value of parameter i.

However, streamflow is not truly a linear function of the parameters in the VIC and routing models. Therefore, a verification run of VIC and the routing model must be performed in order to assess whether the SRTC estimation is accurate. Also, this calibration method finds the best calibrated parameters at a particular station, when this may not be accurate across the entire watershed.

4.4. Model Calibration and Verification

This study is focused on predicting the naturalized, unregulated flows into the Highland Lakes, specifically into Lakes Buchanan and Travis. Since the LCRA has records of inflows into both lakes dating back to 1940, these records are used to calibrate the VIC model based on 1) inflows into Lake Buchanan and 2) the incremental flows below Lake Buchanan and into Lake Travis. In Chapter 5, only forecasts of combined inflows into both lakes will be evaluated.

Xue et al. (2015) found that calibration improvements are made by calibrating to multiple basins, instead of calibrating to only the watershed outlet. From this reasoning,

the SRTC tool was applied to two separate basins: one to calibrate the model for the Lake Buchanan sub-basin (routing flows to the CRBU station), and another to calibrate the model below Lake Buchanan but above Lake Travis, found by taking the difference of the inflows routed to Lake Buchanan and to Lake Travis (routing flows between the CRTR and CRBU stations, referred to as CRTR-CRBU). As noted, the Lake Buchanan sub-basin consists of 118 grid cells, and the Lake Travis sub-basin (which includes the Lake Buchanan sub-basin) consists of 223 grid cells, resulting in the incremental sub-basin below Lake Buchanan and above Lake Travis containing 105 grid cells. Calibrating the two sub-basins separately should improve the overall calibration by incorporating more degrees of freedom.

To aid in the adjustment of the seven soil parameters selected for calibration (including three soil layer depths), Gao et al. (2010) list bounds for each parameter. The parameter b_{infilt} ranges from greater than 0 to approximately 0.4; the parameter Ds_{max} is based on hydraulic conductivity, and typically ranges from greater than 0 to approximately 30 mm/day; soil depth of each layer typically ranges from 0.1 to 1.5 meters; and *Ws* and *Ds* are fractions ranging from 0 to 1. In order to define the extremities for the SRTC for each parameter, the original gridded values associated with each parameter were multiplied by certain percentage increases and decreases until the bounds for each variable were reached. However, for b_{infilt}, a cap of 0.5 was placed on the values if the percentage increase would surpass a value of 0.5. This allowed for a greater increase in b_{infilt} values per grid cell. The extreme ranges for each parameter were determined to be:

1. b_{infilt}: increase by 700% with a cap of 0.5 for any original values which would surpass 0.5; decrease by 99.99%.
2. *Ds*: increase by 19,900%; decrease by 99.5%.
3. Ds_{max}: increase by 200%; decrease by 100%.
4. *Ws*: increase by 4.17%; decrease by 47%.
5. Soil Depth (all three layers): increase by 100%; decrease by 100%, with the constraint that soil layer 1 is always less than soil layer 2.

For each parameter, the upper and lower extremes were placed as the bounds of a Microsoft Excel® slider bar ranging from 0 to 100, where 50 represents the original parameter's value, and therefore no change. In turn, these slider values are scaled with weights used in Equation (4.4) according to a range from -1 to 1, with -1 referring to a slider value of 0; 0 referring to a slider value of 50; and 1 referring to a slider value of 100. A description of the process in scaling the bounds to the slider values is discussed in Appendix E. This process was required due to limited flexibility in the range of slider values in Microsoft Excel®.

The calibration parameters were then adjusted in the SRTC to improve the results of the initial model (using the clipped watershed extent and the STATSGO database, Table 4.2). Gao et al. (2010) recommended the NSE and the relative error be used as the objective functions for calibration through a trial and error tuning process until the modeled flows match satisfactorily with the observed flows. In this study, maximizing NSE was selected as the objective function, and an optimization was performed with the slider bar values as the variables (changing cells in Microsoft Excel®). The Generalized Reduced Gradient (GRG) Nonlinear method (Lasdon et al. 1978) was used, with a

convergence value of 0.0001, central derivatives, a population size of 100, and utilizing a multi-start technique. Constraints limited the change in the variable according to the 0 to 100 scale on the slider bar. Each optimization was completed with all parameters started at 50 (no change), 0 (all minimum), and 100 (all maximum) to add variability in the multi-start technique. The results of the SRTC tool were then verified by making the appropriate percentage changes to the variables in the soil parameter file and re-running the VIC model and the routing model. For simplicity in scaling, the maximization of each parameter suggested by the SRTC was rounded to the nearest 0.5 slider value.

The NSE was maximized for the two basins using the SRTC tool to calibrate the period of January 1, 1960 through December 31, 1989. The results of the entire calibration process are given in Appendix E. In addition to NSE, the coefficient of determination (r^2), correlation coefficient (r), and the percent bias were calculated. The calibrated soil parameters were then applied to the appropriate grid cells relating to CRBU and CRTR-CRBU. The calibrated grid cells for each basin were combined into one soil file and ran through VIC for a verification. Verification results were computed for the entire time window of January 1, 1940 through December 31, 2011, as well as for January 1, 1960 through December 31, 2011 for comparison. This process was done in order to calibrate the model for a small time period and then to verify over a larger time period.

The initial VIC simulation as well as the verifications were run with a two year spin-up period from January 1, 1938 through December 31, 1939. Since VIC simulations have a low bias compared to the observed values, a percentile matching bias correction is applied to the verification output (see Appendix F for more information on the bias

correction procedure). Final calibration and verification results (following bias correction) are summarized in Table 4.3.

Table 4.3. VIC Calibration (1960-1989) and Verification (1940-1959, 1990-2011) Results by Decade, along with changes in performance metrics compared to Table 4.2.

Decade	r^2	r	NSE	Bias (%)	Δr^2	ΔNSE	ΔBias (%)
1940	0.508	0.712	0.475	-19.5	0.173	0.134	0.212
1950	0.680	0.824	0.650	-27.2	0.059	0.036	0.047
1960	0.708	0.841	0.683	0.429	0.070	0.042	0.055
1970	0.757	0.870	0.653	-3.40	-0.002	-0.001	-0.061
1980	0.807	0.898	0.775	8.06	0.029	0.016	0.067
1990	0.882	0.939	0.871	5.43	0.054	0.029	0.076
2000-2011	0.781	0.884	0.680	32.2	0.024	0.014	0.014
1940-2011	0.724	0.851	0.707	-0.758	0.045	0.027	0.053
1960-2011	0.799	0.894	0.759	8.734			

In comparison to Table 4.2, the majority of the performance metrics improved for most decades. For the entire time period of 1940 through 2011, each statistic increased from the original model using the STATSGO database. It is noted that the values of r^2, r, and NSE are the lowest for the decades 1940 and 1950. This is possibly due to changes in land use and land cover that occurred during the middle of the 20th century (see section 2.2 for specific land uses per sub-basin in the Lower Colorado River watershed). The NLDAS vegetation dataset from the University of Maryland describes land cover changes from 1981 to 1994, and so the land cover in the VIC model does not accurately predict watershed fluxes and runoff in the watershed 30 to 40 years prior. Statistics are improved between 1960 and 2011, with r^2 values above 0.708 (with r above 0.841), and NSE values all above 0.653 in each decade.

Focusing on the latter verification period of 1960 through 2011, the r^2 and NSE values increased overall, with r^2 increasing by 0.075 and NSE increasing by 0.052 when comparing the 1940 through 2011 verification with the 1960 through 2011 verification. The percent bias increased compared to the overall time period because bias correction was applied from 1940 through 2011 (where the percent bias is close to zero). Applying the bias correction procedure for 1960 through 2011 did not improve results significantly, and therefore the bias correction for the entire time period was kept.

Even though it is expected that calibration would increase r^2 and NSE for every decade over both verification periods, the fact that there are some declines in the statistics when compared to Table 4.2 (as evident for the r^2 statistic during the 1970 decade) is not surprising. The SRTC tool was used to calibrate the model for the entire 30-year period of 1960 to 1989. Also, the SRTC assumes linear interactions between the variables. These decreases are expected to be a result from model error in how the calibrated parameters interact non-linearly with each other after their calibrated adjustments were performed.

Chapter 5. Hindcast Results and Discussion

5.1. Hindcast Generation

After calibration and verification, the VIC model was run with climate ensemble hindcasts, developed at the University of Wisconsin Madison, to generate ensemble streamflow hindcasts of seasonal inflows to Lakes Buchanan and Travis. The LCRA has observational inflow data for Lakes Buchanan and Travis dating back to 1940 and extending until 2011, but the VIC meteorological forcings files are limited to 2010. Therefore, the VIC global parameter file was set to simulate forecasts from 1940 through 2010. Before starting the forecast (hindcast) run, a two year spin-up of historical forcings data was implemented, starting the model simulation at January 1938 to ensure accurate modeling of the seasons starting in March 1940. Then, the VIC model was run from 1940 through 2010 on a seasonal basis, analyzing the seasons March, April, May, June (MAMJ); July, August, September, October (JASO); and November, December, January, February (NDJF) separately for each year. After the forecasts and historical flows were routed, the forecast output was compared on a seasonal basis against the observed LCRA flows. In this study, an ensemble of four climate forecasts were input to VIC for each season. A fifth model run used the historical meteorological forcings to simulate the actual conditions to compare against the four forecasts. The model was developed so this historical run saves a "state" file, which includes the values of all physical watershed components and water balance fluxes according to the historical data at the last day of the modeled season. This state file was then defined in the global parameter file to be used to start the simulations for the next four-month season. The fluxes (which contain runoff

and baseflow) from each forecast and historical run were then routed to station CRTR using the routing model on a daily time step, with results aggregated to monthly seasonal time steps. Appendix G presents a flowchart on how this process is implemented.

Climate forecasts for the Lower Colorado River basin were produced at the University of Wisconsin Madison. Historical precipitation, maximum and minimum temperature, and wind speed data were taken from the PRISM climatology data set (Daly et al. 1997) for the Texas Climate Division 6 (Edwards Plateau) spatial extent. These data were then spatially and seasonally aggregated and averaged to match the Lower Colorado River basin extent. Model hindcasts of seasonal precipitation and temperature (corresponding to the aggregated PRISM data) were generated using a statistical forecast model developed at the University of Wisconsin Madison, utilizing the procedure developed by Zimmerman and Block (2015). Using a nearest neighbor approach, ten "analog" years were selected representing the historical years with seasonal precipitation and temperature data matching closest to the forecast values. Finally, individual months were randomly sampled from the set of analog years for the MAMJ and JASO seasons to generate seasonal hindcasts over the time period of 1960 through 2010 (with the ability to go back as far as 1915). Currently, climate forecasts are not generated for the NDJF because this season has the least streamflow variability. A list of the closest analog years for MAMJ from 1960 through 2010 is given in Appendix H.

Results are presented for mean ensemble hindcasts for 152 individual seasons, from MAMJ 1960 through JASO 2010, using four hindcasts. The meteorological forcings for the four hindcasts as well as the script used to loop the hindcasts through the three seasons are included in the "01Model" folder in the supplemental materials.

5.2. Hindcast Results and Analysis

In order to compare each hindcast to the historical predicted flows from VIC as well as the LCRA's observed inflows to Lake Travis, the mean of the four monthly ensemble hindcasts is evaluated for each month, and a percentile-matching bias correction procedure is applied. Because the hindcast forcings were generated on a seasonal basis and the model is for seasonal streamflow forecasting, the ensemble monthly mean hindcast flows are also analyzed by season. The ensemble mean hindcasts averages are sorted according to each season, where total seasonal flows are calculated and analyzed. The NDJF season is not reported in this section, because this season sees less variability in streamflow, and hydrologic persistence serves as a skillful predictor.

A comparison of the full time series of monthly ensemble mean hindcasts to the LCRA observed inflows is given in Figure 5.1. It is evident that the hindcasts have a low bias in comparison to the peak observed inflows; though, it is expected that an ensemble mean will not accurately capture the extreme high or low values. A scatterplot of these flows, showing the variance between the monthly hindcasts and the monthly LCRA observed flows, is given in Figure 5.2, with statistics presented in Table 5.1.

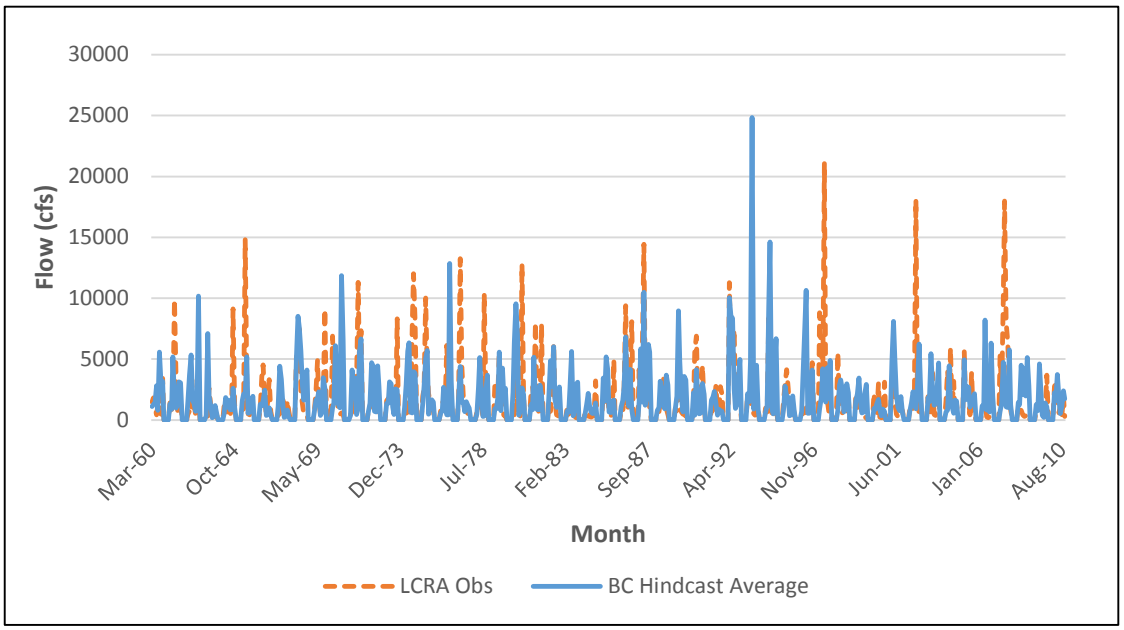

Figure 5.1. Comparison of Ensemble Mean Hindcasts (MAMJ and JASO) to the LCRA Observed Inflows to Lake Travis, March 1960 through October 2010. Ensemble mean hindcasts are bias corrected. Created by author.

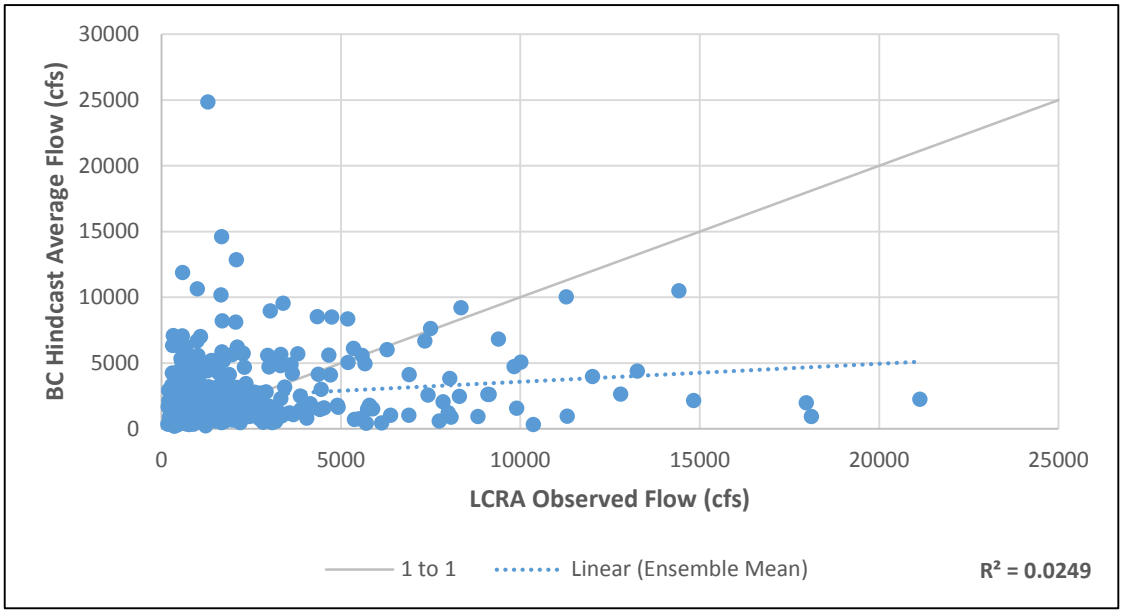

Figure 5.2. Scatterplot of the Ensemble Mean Hindcasts (MAMJ and JASO) versus the LCRA Observed Inflows to Lake Travis, March 1960 to October 2010. Ensemble mean hindcasts are bias corrected. Created by author.

Figures 5.3 and 5.4 show the distribution of seasonal ensemble mean hindcasts compared to the LCRA's total seasonal observed inflows for the seasons MAMJ and JASO, respectively. Statistics for these comparisons are also presented in Table 5.1.

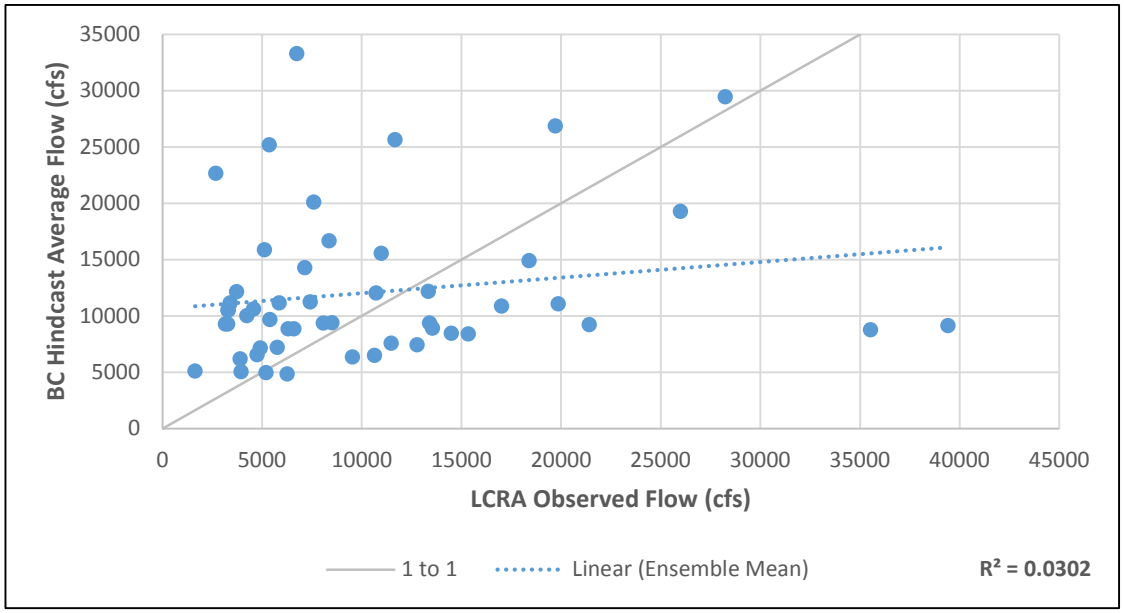

Figure 5.3. MAMJ Ensemble Mean Hindcasts and LCRA Observed Inflows to Lake Travis, 1960-2010. Ensemble mean hindcasts are bias corrected. Created by author.

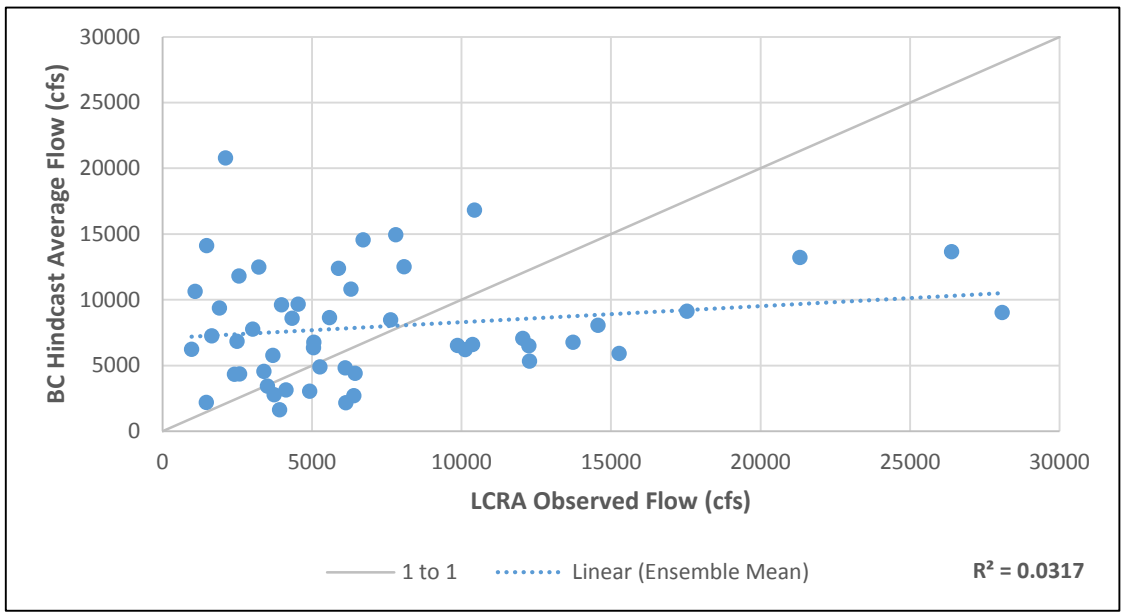

Figure 5.4. JASO Ensemble Mean Hindcasts and LCRA Observed Inflows to Lake Travis, 1960-2010. Ensemble mean hindcasts are bias corrected. Created by author.

Table 5.1. Seasonal Statistics of Ensemble Mean Hindcasts compared to LCRA Observed Inflows to Lake Travis from 1960 to 2010.

Season	r^2	r	**NSE**
MAMJ	0.030	0.174	-0.381
JASO	0.032	0.178	-0.236
Overall	0.025	0.158	-0.489

Besides comparing the four ensemble mean hindcasts to the LCRA observed inflows, it is important to assess the variability between the seasonal ensemble mean hindcasts and historical simulated flows. The simulated inflows calculated using the historical forcings from Livneh et al. (2013) during calibration and verification are compared to the ensemble mean hindcasts. Figure 5.5 presents the overall time series of the average monthly hindcast flows compared to the historical simulated flows, with Figure 5.6 showing a scatterplot to represent the variance. Figures 5.7 and 5.8 present the overall time series and seasonal comparisons of the ensemble mean hindcasts to the historical simulated flows, with associated statistics given in Figure 5.2.

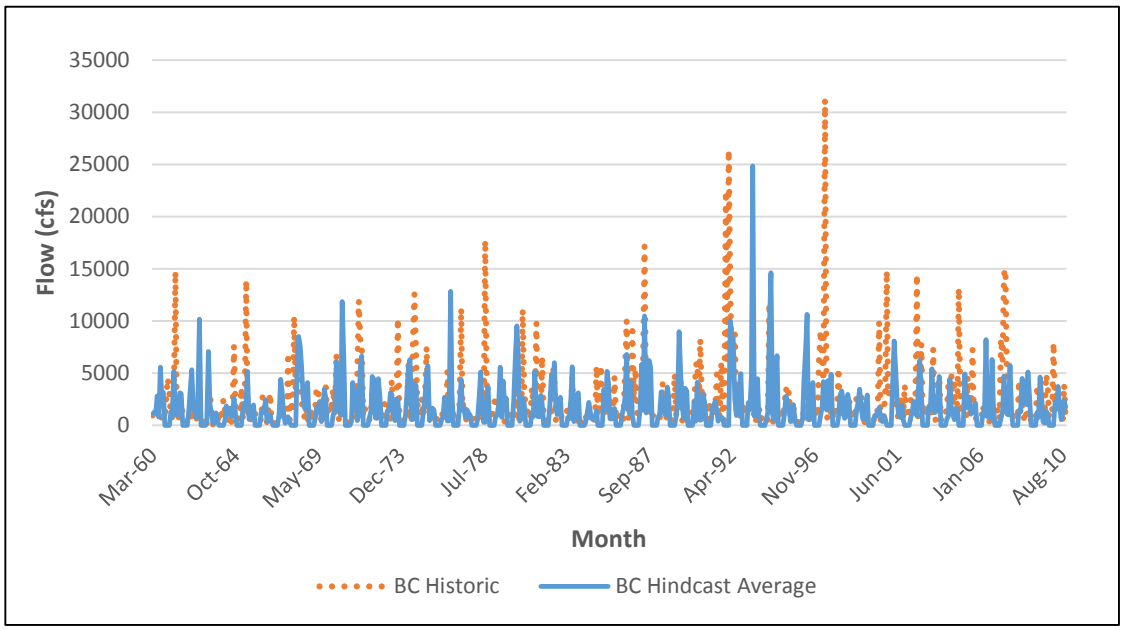

Figure 5.5. Comparison of Ensemble Mean Hindcasts to the Historical Simulation (MAMJ AND JASO) of Inflows to Lake Travis, March 1960 through October 2010. Both ensemble mean hindcasts and historical simulations are bias corrected. Created by author.

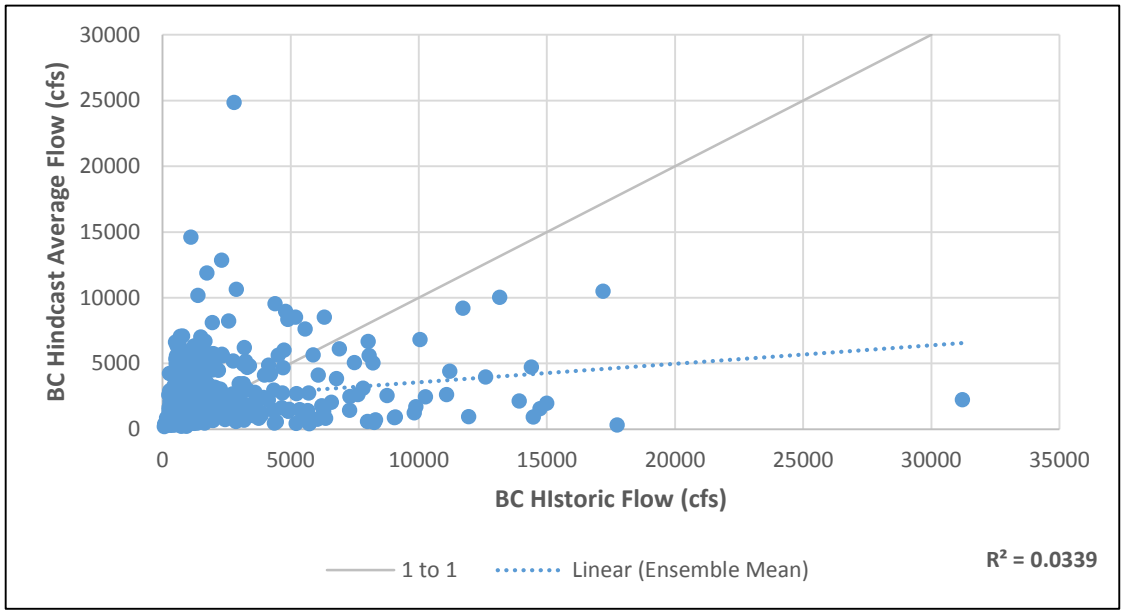

Figure 5.6. Scatterplot of the Ensemble Mean Hindcasts (MAMJ and JASO) versus the Historical Simulation of Inflows to Lake Travis, March 1960 through October 2010. Both ensemble mean hindcasts and historical simulations are bias corrected. Created by author.

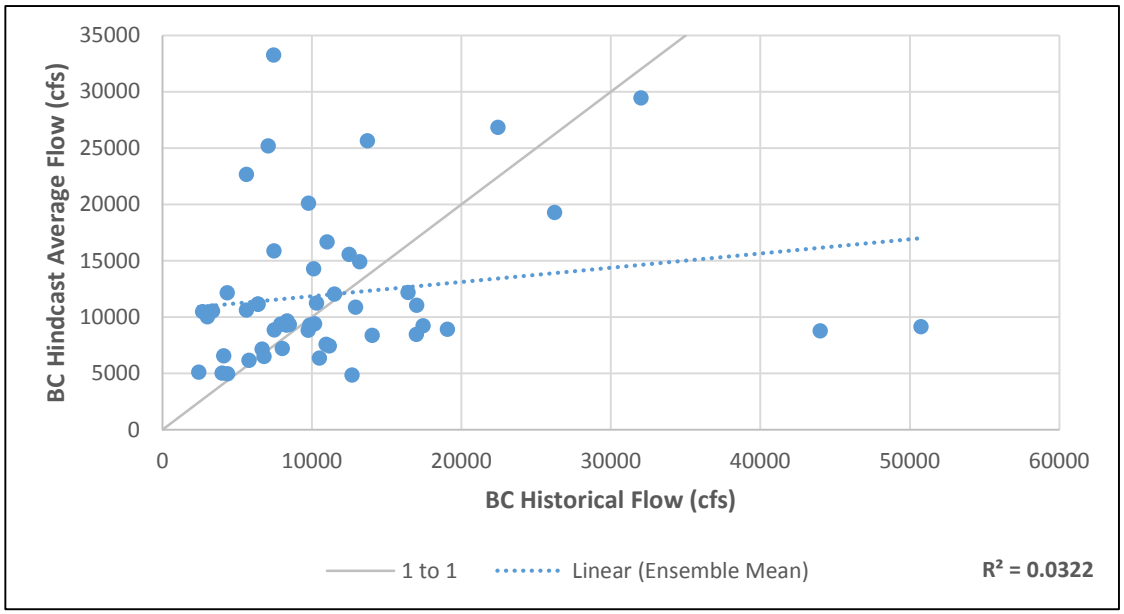

Figure 5.7. MAMJ Ensemble Mean Hindcasts versus Historical Simulation of inflows to Lake Travis, 1960-2010. Both ensemble mean hindcasts and historical simulations are bias corrected. Created by author.

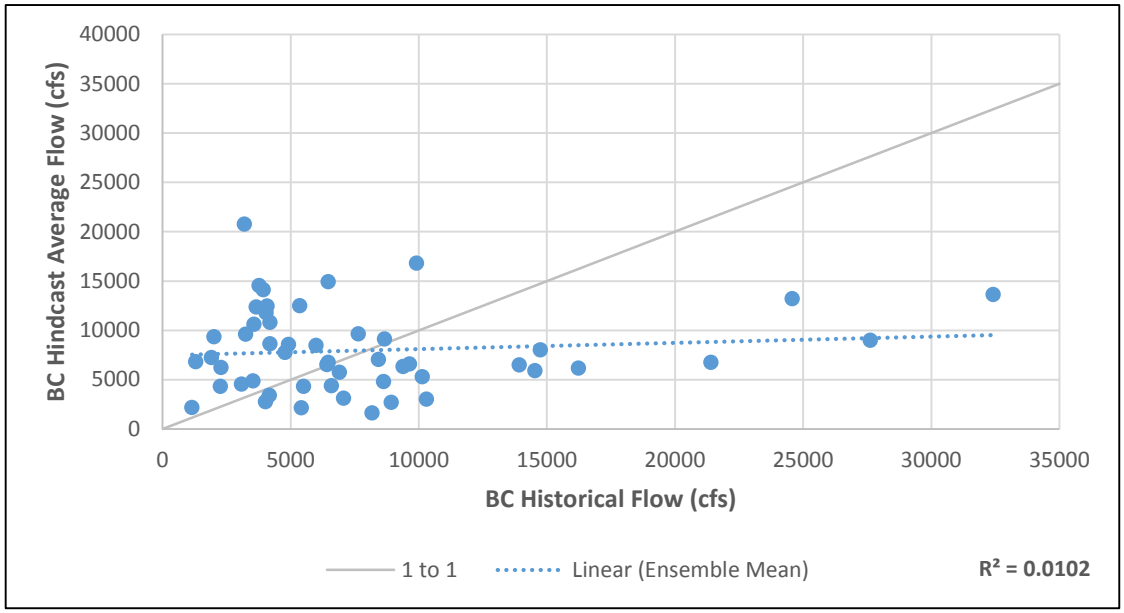

Figure 5.8. JASO Ensemble Mean Hindcasts versus Historical Simulation of inflows to Lake Travis, 1960-2010. Both ensemble mean hindcasts and historical simulations are bias corrected. Created by author.

Table 5.2. Seasonal Statistics of Ensemble Mean Hindcasts compared to Historical Simulation of Inflows to Lake Travis.

Season	r^2	r	NSE
MAMJ	0.032	0.180	-0.241
JASO	0.010	0.101	-0.267
Overall	0.034	0.184	-1.23

5.3. Diagnosis of Forecast Skill

Results for the MAMJ and JASO seasons evaluated from 1960 to 2010 indicate virtually no skill in the season-ahead inflow hindcasts, despite significant skill in the precipitation hindcasts ($r^2 > 0.5$ for the MAMJ and JASO seasons) and reasonably good calibration and verification statistics for the VIC model (see Chapter 4). Comparing monthly VIC output to the LCRA observed inflows into Lake Travis over the entire time period using the hindcasts, $r^2 = 0.799$ and NSE = 0.759. These statistics were computed using a continuous run and analyzed by decade; when the calibrated model was run using the seasonal procedure, $r^2 = 0.827$ for the MAMJ season and $r^2 = 0.763$ for the JASO season when compared to the LCRA observed inflows (graphics are given in Appendix E). However, when the ensemble mean hindcasts are compared to the LCRA observed inflows, r^2 decreases to 0.030 for the MAMJ season and to 0.174 for the JASO season. The NSE also decreases to -0.381 and -0.236 for the MAMJ and JASO seasons, respectively (see Table 5.1).

The study conducted by Sinha and Sankarasubramanian (2013) is similar to this research in that the skill of seasonal forecasts is calculated from ensemble mean forecast simulations from VIC for the Apalachicola River in Chattaoochee, Florida. Results from forecasts with times from 1 to 6 months reveal correlations and accuracy fluctuate over

increasing lead times, and results have very low correlation and accuracy in August, despite very high correlations during the verification period. Since Sinha and Sankarasubramanian (2013) also found low skill and correlation in seasonal ensemble predictive forecasts after a proper calibration, the results of low forecast skill in this study are not as striking. However, it is still important to diagnose the cause of the low skill.

Three reasons are proposed for the lack of skill in the inflow hindcasts, investigated herein. First, the use of meteorological data for the Texas Climate Division 6, rather than the Lower Colorado River basin area draining to Lake Travis (CRTR), may introduce some variability in the climate forecasts. Second, the downscaling method, which selects analogs based on a nearest neighbors approach, can add variability and degrade forecast skill. Third, soil moisture may not be strongly correlated with observed flows, and the soil moisture "state" may not influence streamflow on a seasonal timescale. In addition to these potential errors, hydrologic model error will also contribute to low skill in season-ahead inflow forecasts.

The low skill in the ensemble mean hindcasts was diagnosed. First, annual precipitation values corresponding to the Texas Climate Division 6 and the Lower Colorado River basin (draining into Lake Travis) were compared. Since the PRISM data used to generate the hindcasts were not readily available from the University of Wisconsin Madison for this analysis, precipitation data were obtained from the National Centers for Environmental Prediction/National Center for Atmospheric Research (NCEP/NCAR) reanalysis dataset (Kalnay et al. 1996). Meteorological data for the Texas Climate Division 6 extent were taken from coordinates (30.0 to 32.5° N, 97.5 to 102.5° W); this is the same area used to obtain precipitation and temperature data from PRISM

for the hindcasts. Precipitation data were also taken from a smaller area, (30.0625 to 32.3125° N, 97.9375 to 100.5625° W), representing the Lake Travis drainage basin. For the MAMJ season, the average areal precipitation was 255.8 mm over the Texas Climate Division 6 area and 324.3 mm over the Lower Colorado River basin, for the years 1948 to 2011. In comparison, the average areal precipitation from the PRISM dataset used in the hindcasts is 234.6 mm. The similar average areal precipitation values between the PRISM and NCEP/NCAR data sets from (30.0 to 32.5° N, 97.5 to 102.5° W) indicates that the PRISM dataset (used to generate the precipitation hindcasts) was taken from the Texas Climate Division 6 area. When comparing the PRISM dataset over the Climate Division 6 area to the precipitation data over the Lake Travis drainage area from NCEP/NCAR, there is a 27.7% difference in the average areal precipitation values. Despite the difference in the average areal precipitation between the two areas, the correlation of precipitation between the two areas is very high, at $r^2 = 0.955$, indicating that this is not a primary reason for low forecast skill. However, the precipitation hindcasts (using PRISM data over the Texas Climate Division 6) have significantly lower correlation to the observed NCEP precipitation over the LCRA managed area, which perhaps indicates that the precipitation forecast model is not very robust. These results are given in Table 5.3.

Table 5.3. Coefficient of Determination (r^2) Matrix of Precipitation data and Hindcasts for the season MAMJ, 1948-2010.

	Hindcast Model	NCEP (Climate Division 6)	NCEP (CRTR)
NCEP (Climate Division 6)	0.366		
NCEP (CRTR)	0.347	0.955	
PRISM	0.547	0.675	0.619

Next, the correlation between precipitation and streamflow data was examined, to determine whether or not a different precipitation data set should be used to generate the forecasts. The PRISM precipitation data used in the hindcasts (historical precipitation data) correlates strongly with the historically observed inflows to Lake Travis, at r^2 = 0.599 (this is shown in Table 5.4). In turn, the hindcast model, which predicts a season-ahead, predicts the actual PRISM precipitation data at r^2 = 0.547 (Table 5.3). The variability in both sets is additive when the precipitation hindcast model directly predicts streamflow, resulting in a lower coefficient of determination, at r^2 = 0.298. This error propagation could be one reason for the degradation of streamflow forecasts, as uncertainties associated with variables interact. Correlations between each precipitation dataset and the observed inflows are given in Table 5.4. The observed inflows correlate best to the Texas Climate Division 6 area with the PRISM data at r^2 = 0.599, supporting that these data are appropriate for use in the forecast model.

Table 5.4. Coefficient of Determination (r^2) of the Precipitation and Hindcasts to the Observed Inflows to Lake Travis for the season MAMJ, 1948-2010

	Observed Inflows
NCEP (Climate Division 6)	0.538
NCEP (CRTR)	0.516
PRISM	0.599
Hindcasts	0.298

The second diagnostic analysis examined how the hindcast generation technique—specifically the downscaling method—affects streamflow predictions. Following the nearest-neighbor sampling procedure (Zimmerman and Block 2015), NCEP/NCAR precipitation data were randomly selected for each month from the analog years corresponding to each MAMJ hindcast. Over the Texas Climate Division 6 extent, the downscaled precipitation correlates to the actual NCEP/NCAR precipitation data at $r^2 = 0.420$, while for the Lake Travis basin, $r^2 = 0.399$. When comparing the downscaled precipitation forecasts to the observed inflows, $r^2 = 0.202$ for precipitation data from the Texas Climate Division 6 area, and $r^2 = 0.147$ for precipitation data from the LCRA managed area. In comparison to the correlation of the actual PRISM data to the observed inflows ($r^2 = 0.599$), the downscaling process appears to degrade the forecast skill.

Lastly, the relative influence of soil moisture on streamflow was analyzed. One hypothesis of this study is that observed soil moisture combined with seasonal precipitation forecasts would improve streamflow predictions over either variable alone. For this reason, the VIC model saves the watershed "state" at the end of each season to use in the next seasonal forecast. Soil moisture input is from the NLDAS dataset. Soil

moisture data over a depth from 0 to 100 centimeters were analyzed over the Lower Colorado River basin (30.0 to 32.5° N, -97.5 to 102.5° W) for the period 1979 to 2010. For the seasons MAMJ and JASO, the correlation between soil moisture and the concurrent observed inflows is $r^2 = 0.229$. In addition, soil moisture has a high autocorrelation with a one month lag, at $r^2 = 0.764$, indicating that it may be useful as a predictor variable. However, this autocorrelation drops rapidly after four months to $r^2 = 0.085$. This reveals soil moisture at the end of the previous season is not a good predictor for the next season. Soil moisture also does not correlate well to observed inflows lagged at one month ($r^2 = 0.061$), indicating the watershed soil moisture state does not highly influence the next month's streamflow. These statistics are represented in Figure 5.9.

The relationship between streamflow and soil moisture appears to be non-linear. The amount of soil moisture required for saturation is dependent on soil texture and thickness, and the volume of streamflow is dependent on the volume of runoff produced. Soils exhibit a threshold in saturation which dictates the initiation of different forms of overland flow. The volume of runoff varies from soil response and type of overland flow processes, precipitation intensity and volume, among other external factors. These factors support the non-linear response observed in Figure 5.9. Quadratic and power regressions were also computed to support this non-linear response. The r^2 statistic increased to $r^2 = 0.342$ using a quadratic regression and to $r^2 = 0.455$ using a power regression. However, as seen in Figures 5.10 and 5.11, these regressions still cannot accurately simulate the high flows in the non-linear interaction between streamflow and soil moisture.

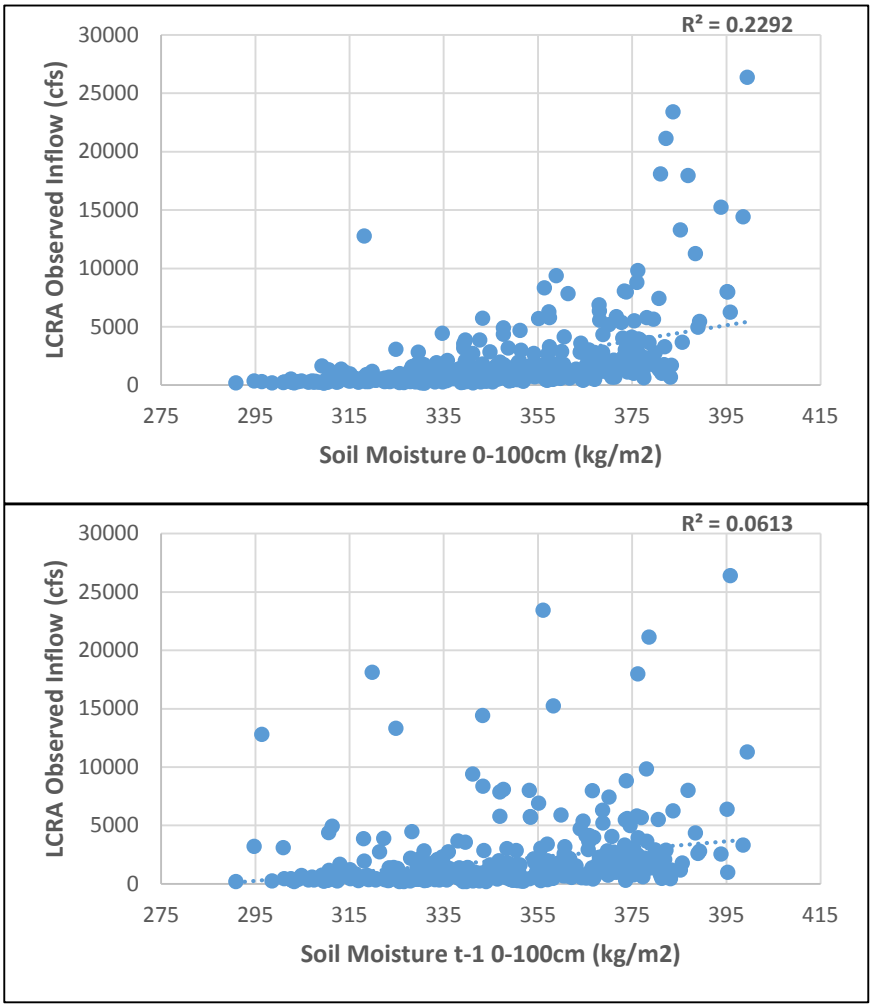

Figure 5.9. Relationships between Soil Moisture and LCRA Observed Inflows with and without a Time Lag for the MAMJ and JASO seasons, 1979-2010. Created by author.

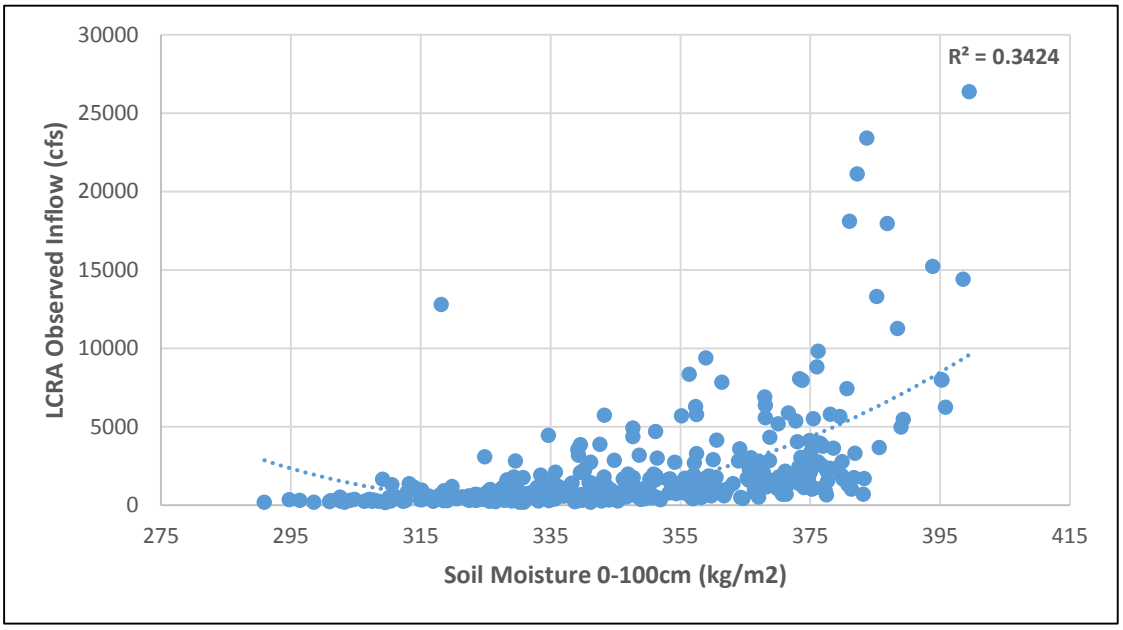

Figure 5.10. Quadratic Regression of Soil Moisture and LCRA Observed Inflows for the MAMJ and JASO seasons, 1979-2010. Created by author.

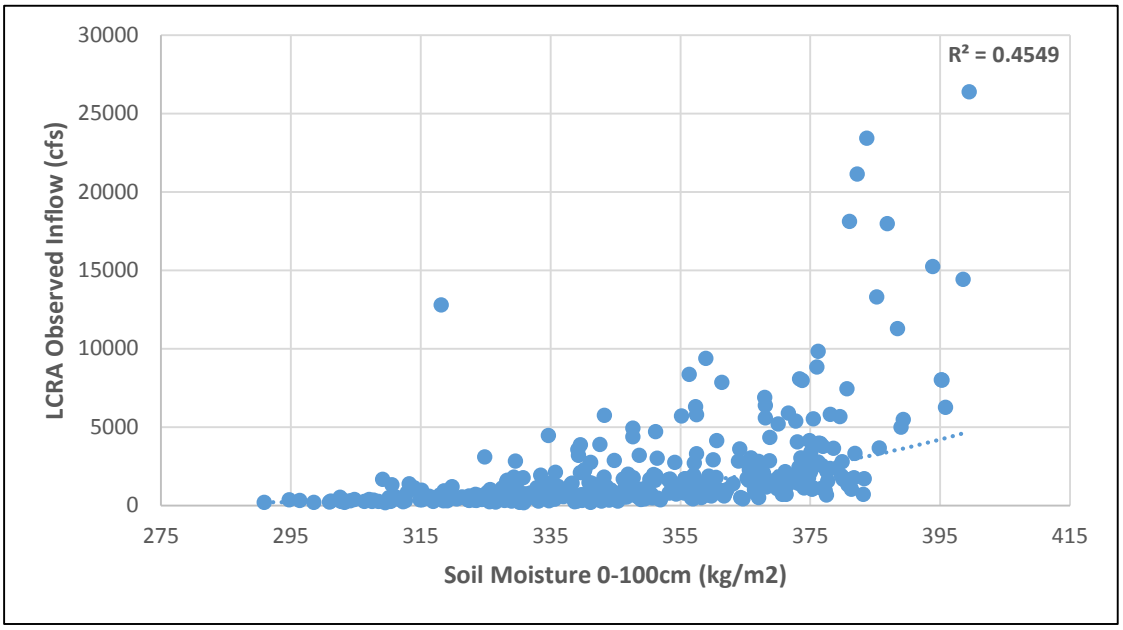

Figure 5.11. Power Regression of Soil Moisture and LCRA Observed Inflows for the MAMJ and JASO seasons, 1979-2010. Created by author.

In conclusion, the precipitation data used in the forecast model are found to be accurate, but the downscaling process should be revised in order to produce more skillful streamflow forecasts. Also, using the soil moisture "state" prior to a season has been found to not be as influential as expected. Improved soil moisture data, including *in situ* soil moisture measurements and high-resolution satellite-based observations, which can better represent variability in soil moisture, may also help in the seasonal prediction of streamflow.

Chapter 6. Conclusions and Future Work

6.1. Conclusions

This study developed a calibrated, physically-based watershed model for the Lower Colorado River basin for the purpose of season-ahead forecasting for the LCRA. This model couples the VIC land surface hydrology model with an associated routing model to route streamflow through the Lake Buchanan and Lake Travis sub-watersheds in the Lower Colorado River basin on a 1/8° grid. The model is physically-based through the incorporation of elevation bands and vegetation cover using the NLDAS data sets, and three soil layer depths representing spatial variability using the STATSGO database. The model uses forecasted meteorological forcings in order to calculate water and energy balances in the watershed.

The model has been calibrated by adjusting seven soil parameters for individual grid cells in the Lake Buchanan basin and the sub-basin below Lake Buchanan and above Lake Travis. The calibration was completed over the time period 1960 to 1989, and the model was then verified over the entire time period of 1940 to 2010. Verification results were analyzed by decade, revealing r^2 values ranging from 0.708 in the 1960s to 0.882 in the 1990s. The NSE for these decades ranged between 0.655 in the 1970s and to 0.872 in the 1990s.

The overall objective of the research was to calibrate and diagnose seasonal hindcasts using this developed watershed model. This study tested the meteorological inputs associated with four preliminarily created hindcasts, in order to assess the accuracy of the VIC and routing model in matching predicted inflows to observed inflows between

1940 and 2010. The four generated hindcasts tested in this study revealed poorly correlated (and therefore, not skilled) forecasts, resulting in poor correlations of seasonal r^2 and NSE values for the MAMJ and JASO seasons when compared to the LCRA observed inflows, as well as when compared to the predicted inflows from historical meteorological data. Diagnosis of the unskilled forecasts determined that precipitation inputs highly correlate to the observed inflows, but the downscaling technique degrades the forecasts significantly. Also, the soil moisture "state" is found to not be as influential producing the season-ahead streamflow as originally expected. However, the physically-based VIC model was developed appropriately for the LCRA management extent to generate forecasts as determined in the verification stage, and is now available for future use as the study progresses in order to develop skillful forecasts once appropriate meteorological forcings are generated.

6.2. Future Work

There are several steps to be completed in order to generate more skillful seasonal forecasts for the LCRA. The next focus is to improve the precipitation forecasts over the Lower Colorado River basin. The meteorological data, which serves as the basis for the forecasts, should correspond to the basin above Lake Travis rather than the Texas Climate Division 6 applied to the Lower Colorado River basin to more accurately represent the average areal precipitation driving inflows to the reservoirs. The downscaling procedure for developing daily gridded inputs to the VIC model needs to be analyzed in more detail and possibly improved. Finally, the forecast ensemble will be increased in size to better represent the uncertainty in climate forecasts. The physically-

based hydrologic forecasts will be combined with statistical climate forecasts generated at Columbia University, linking GCMs with the physical watershed components to create a hydroclimatic forecasting model.

Additional work is needed to incorporate soil moisture measurements in the VIC model. *In situ* soil moisture measurements conducted by the Michigan Tech Research Institute (MTRI) have been collected from soil moisture gauges and remote sensing observations. These data can be assimilated in the VIC model to represent physical soil moisture in the state file at the beginning of each forecast period.

The ultimate goal of this work is to allow the LCRA to incorporate seasonal forecasts in future water management plans. The hydroclimatic forecast model will combine with the stochastic optimization model at the University of Wisconsin Madison in order to develop future outcomes and impacts, and will allow the LCRA to revise operating rules. The model will be run for short-term and seasonal forecasting to be incorporated into the LCRA's decision support system (DSS) to define drought triggers, identify potential future curtailment, assist in irrigation scheduling, and maintain environmental flows.

The final model, when coupled with the DSS, will help to identify and mitigate against risk associated with a poor forecast. Risks and benefits for individual stakeholders will be evaluated if a drought trigger is forecasted, as operation decisions may need to be shifted. The LCRA can use the climate forecasts to determine if equitable allocation of risks and benefits between stakeholders is necessary.

References

Abdulla, F. A., Lettenmaier, D. P., Wood, E. F., and Smith, J. A. (1996). "Application of a macroscale hydrologic model to estimate the water balance of the Arkansas-Red River Basin." *Journal of Geophysical Research*, 101(D3), 7449-7459.

Acharya, A., Piechota, T. C., and Tootle, G. (2012). "Quantitative Assessment of Climate Change Impacts on the Hydrology of the North Platte River Watershed, Wyoming." *Journal of Hydrologic Engineering*, 17(10), 1071-1083.

Andreadis, K. M., and Lettenmaier, D. P. (2006). "Trends in 20th century drought over the continental United States." *Geophysical Research Letters*, 33(10).

Ashofteh, P. S., Bozorg Haddad, O., and Mariño, M. A. (2013). "Scenario Assessment of Streamflow Simulation and its Transition Probability in Future Periods Under Climate Change." *Water Resources Management*, 27(1), 255-274.

Beyene, T., Lettenmaier, D. P., and Kabat, P. (2009). "Hydrologic impacts of climate change on the Nile River Basin: implications of the 2007 IPCC scenarios." *Climatic Change*, 100(3-4), 433-461.

Cai, X., Zeng, R., Kang, W. H., Song, J., and Valocchi, A. J. (2015). "Strategic Planning for Drought Mitigation under Climate Change." *Journal of Water Resources Planning and Management*, 04015004.

CH2M HILL (2008). "Climate Change Study: Report on Evaluation Methods and Climate Scenarios."Submitted to Lower Colorado River Authority and San Antonio Water System, TX, 103.

CHI Support (2015). "Calibrating a SWMM5 model using the SRTC tool." <http://support.chiwater.com/support/solutions/articles/29894-calibrating-a-swmm5-model-using-the-srtc-tool>. (October, 2015).

Daly, C., Halbleib, M., Smith, J. I., Gibson, W. P., Doggett, M. K., Taylor, G. H., Curtis, J., and Pasteris, P. P. (2008). "Physiographically sensitive mapping of climatological temperature and precipitation across the conterminous United States." *International Journal of Climatology*, 28(15), 2031-2064.

Daly, C., Neilson, R. P., and Phillips, D. L. (1994). "A Statistical-Topographic Model for Mapping Climatological Precipitation over Mountainous Terrain." *Journal of Applied Meteorology*, 33(2), 140-158.

Daly, C., Taylor, G., and Gibson, W. (1997). "The Prism Approach to Mapping Precipitation and Temperature." Oregon State University.

Day, G. N. (1985). "Extended Streamflow Forecasting Using NWSRFS." *Journal of Water Resources Planning and Management*, 111(2), 157-170.

Dracup, J. A., Lee, K. S., and Paulson, E. G., Jr. (1980b). "On the Definition of Droughts." *Water Resources Research*, 16(2), 297-302.

Faber, B. A., and Stedinger, J. R. (2001). "Reservoir optimization using sampling SDP with ensemble streamflow prediction (ESP) forecasts." *Journal of Hydrology*, 149(1), 113-133.

Franchini, M., and Pacciani, M. (1991). "Comparative analysis of several conceptual rainfall-runoff models." *Journal of Hydrology*, 122(1), 161-219.

Gao, H., Tang, Q., Shi, X., Zhu, C., Bohn, T. J., Su, F., Sheffield, J., Pan, M., Lettenmaier, D. P., and Wood, E. F. (2010). "Water budget record from Variable

Infiltration Capacity (VIC) model." *Algorithm Theoretical Basis Document for Terrestrial Water Cycle Data Records*, (Unpublished).
Hallack-Alegria, M., and Watkins, D. W., Jr. (2005). "Drought Frequency Analysis and Prediction in Sonora, Mexico." Michigan Technological University, Department of Civil and Environmental Engineering.
Hamlet, A. F., and Lettenmaier, D. P. (1999). "Columbia River Streamflow Forecasting Based on ENSO and PDO Climate Signals." *Journal of Water Resources Planning and Management*, 125(6), 333-341.
Heim, R. R., Jr. (2002). "A Review of Twentieth-Century Drought Indices Used in the United States." *Bulletin of the American Meteorological Society*, 83(8), 1149-1165.
Heo, J., Yu, J., Giardino, J. R., and Cho, H. (2015). "Impacts of climate and land-cover changes on water resources in a humid subtropical watershed: a case study from East Texas, USA." *Water and Environment Journal*, 29(1), 51-60.
Kalnay, E., Kanamitsu, M., Kistler, R., Collins, W., Deaven, D., Gandin, L., Iredell, M., Saha, S., White, G., Woollen, J., Zhu, Y., Chelliah, M., Ebisuzaki, W., Higgins, W., Janowiak, J., Mo, K. C., Ropeleweski, C., Wang, J., Leetmaa, A., Reynolds, R., Jenne, R., and Joseph, D. (1996). "The NCEP/NCAR 40-Year Reanalysis Project." *Bulletin of the American Meteorological Society*, 77(3), 437-471.
Kracman, D. R., McKinney, D. C., Watkins, D. W., Jr., and Lasdon, L. S. (2006). "Stochastic Optimization of the Highland Lakes System in Texas." *Journal of Water Resources Planning and Management*, 132(2), 62-70.
Lasdon, L. S., Waren, A. D., Jain, A., and Ratner, M. (1978). "Design and Testing of a Generalized Reduced Gradient Code for Nonlinear Programming." *ACM Transactions on Matematical Software (TOMS)*, 4(1), 34-50.
LCRA (2006). "Colorado River Basin Watersheds." Map.
LCRA (2010). "Water Management Plan for the Lower Colorado River Basin." Lower Colorado River Authority, Austin, TX.
LCRA (2015a). "Historic drought and the lower Colorado River basin."Austin, TX.
LCRA (2015b). "How the Highland Lakes work."Austin, TX.
LCRA (2015c). "Buchanan Dam and Lake Buchanan."
LCRA (2015d). "Mansfield Dam and Lake Travis."
Liang, X., Lettenmaier, D. P., Wood, E. F., and Burges, S. J. (1994). "A simple hydrologically based model of land surface water and energy fluxes for general circulation models." *Journal of Geophysical Research*, 99(D7), 14,415-414,428.
Livneh, B., Rosenberg, E. A., Lin, C., Nijssen, B., Mishra, V., Andreadis, K. M., Maurer, E. P., and Lettenmaier, D. P. (2013). "A Long-Term Hydrologically Based Dataset of Land Surface Fluxes and States for the Conterminous United States: Update and Extensions*." *Journal of Climate*, 26(23), 9384-9392.
Lohmann, D., Nolte-Holube, R., and Raschke, E. (1996). "A large-scale horizontal routng model to be coupled to land surface parameterization schemes." *Tellus A*, 48(5), 708-721.
Lohmann, D., Raschke, E., Nijssen, B., and Lettenmaier, D. P. (1998a). "Regional scale hydrology: I. Formulation of the VIC-2L model coupled to a routing model." *Hydrological Sciences Journal*, 43(1), 131-141.

Lohmann, D., Raschke, E., Nijssen, B., and Lettenmaier, D. P. (1998b). "Regional scale hydrology: II. Application of the VIC-2L model to the Weser River, Germany." *Hydrological Sciences Journal*, 43(1), 143-158.

Luo, L., and Wood, E. F. (2007). "Monitoring and predicting the 2007 U.S. drought." *Geophysical Research Letters*, 34(22).

Maurer, E. P., Wood, A. W., Adam, J. C., Lettenmaier, D. P., and Nijssen, B. (2002). "A Long-Term Hydrologically Based Dataset of Land Surface Fluxes and States for the Conterminous United States*." *Journal of Climate*, 15(22), 3237-3251.

McKee, T. B., Doesken, N. J., and Kleist, J. (1993). "The Relationship of Drought Frequency and Duration to Time Scales." *Eighth Conference on Applied Climatology* Anaheim, CA, 179-184.

Mitchell, K. E. (2004). "The multi-institution North American Land Data Assimilation System (NLDAS): Utilizing multiple GCIP products and partners in a continental distributed hydrological modeling system." *Journal of Geophysical Research*, 109(D7).

Mozny, M., Trnka, M., Zalud, Z., Hlavinka, P., Nekovar, J., Potop, V., and Virag, M. (2012). "Use of a soil moisture network for drought monitoring in the Czech Republic." *Theoretical and Applied Climatology*, 107(1-2), 99-111.

Nalbantis, I., and Tsakiris, G. (2009). "Assessment of Hydrological Drought Revisited." *Water Resources Management*, 23(5), 881-897.

NASA (2015a). "NLDAS Vegetation Class/Mask." <http://ldas.gsfc.nasa.gov/nldas/NLDASvegetation.php>. (October, 2015).

Nijssen, B., Lettenmaier, D. P., Liang, X., Wetzel, S. W., and Wood, E. F. (1997). "Streamflow simulation for continental-scale river basins." *Water Resources Research*, 33(4), 711-724.

Palmer, W. C. (1965). "Meteorological Drought. Research Paper No. 45." U. S. W. Bureau, ed., U.S. Government Printing Office, Washington, D.C.

Pennsylvania State University (1998). "Soil Information for Environmental Modeling and Ecosystem Management." <http://www.soilinfo.psu.edu/index.cgi?soil_data&statsgo>. (October, 2015).

Qiao, L., Hong, Y., McPherson, R., Shafer, M., Gade, D., Williams, D., Chen, S., and Lilly, D. (2014). "Climate Change and Hydrological Response in the Trans-State Oologah Lake Watershed-Evaluating Dynamically Downscaled NARCCAP and Statistically Downscaled CMIP3 Simulations with VIC Model." *Water Resources Management*, 28(10), 3291-3305.

Ryu, J. H., Sohrabi, M., and Acharya, A. (2014). "Toward Mapping Gridded Drought Indices to Evaluate Local Drought in a Rapidly Changing Global Environment." *Water Resources Management*, 28(11), 3859-3869.

Seager, R., Hoerling, M., Schubert, S., Wang, H., Lyon, B., Kumar, A., Nakamura, J., and Henderson, N. (2015). "Causes of the 2011-14 California Drought*." *Journal of Climate*, 28(18), 6997-7024.

Senay, G. B., Budde, M. E., Brown, J. F., and Verdin, J. P. "Mapping Flash Drought in the U.S. Southern Great Plains." *Proc., 22nd Conference on Hydrology*.

Sharma, T. C., and Panu, U. S. (2012). "Prediction of hydrological drought durations based on Markov chains: case of the Canadian prairies." *Hydrological Sciences Journal*, 57(4), 705-722.

Sheffield, J., Andreadis, K. M., Wood, E. F., and Lettenmaier, D. P. (2009). "Global and Continental Drought in the Second Half of the Twentieth Century: Severity–Area–Duration Analysis and Temporal Variability of Large-Scale Events." *Journal of Climate*, 22(8), 1962-1981.

Sheffield, J., Goteti, G., Wen, F., and Wood, E. F. (2004a). "A simulated soil moisture based drought analysis for the United States." *Journal of Geophysical Research*, 109(D24108).

Sheffield, J., and Wood, E. F. (2007). "Characteristics of global and regional drought, 1950–2000: Analysis of soil moisture data from off-line simulation of the terrestrial hydrologic cycle." *Journal of Geophysical Research*, 112(D17).

Sheffield, J., and Wood, E. F. (2008). "Projected changes in drought occurrence under future global warming from multi-model, multi-scenario, IPCC AR4 simulations." *Climate Dynamics*, 31(1), 79-105.

Shepard, D. S. (1984). "Computer Mapping: The SYMAP Interpolation Algorithm." *Spatial Statistics and Models*, G. L. Gaile, and C. J. Willmott, eds., Springer Netherlands, 133-145.

Shukla, S., Steinemann, A. C., and Lettenmaier, D. P. (2011). "Drought Monitoring for Washington State: Indicators and Applications." *Journal of Hydrometeorology*, 12(1), 66-83.

Sinha, T., and Sankarasubramanian, A. (2013). "Role of climate forecasts and initial conditions in developing streamflow and soil moisture forecasts in a rainfall–runoff regime." *Hydrology and Earth System Sciences*, 17(2), 721-733.

Smith, J. A., Day, G. N., and Kane, M. D. (1992). "Nonparametric Framework for Long-Range Streamflow Forecasting." *Journal of Water Resources Planning and Management*, 118(1), 82-92.

Smith, R. K. (2015). "Changing rainfall and humidity within Southeast Texas." *SpringerPlus*, 4(1), 1-11.

Stamm, J. F., Wood, E. F., and Lettenmaier, D. P. (1994). "Sensitivity of a GCM Simulation of Global Climate to the Representation of Land-Surface Hydrology." *Journal of Climate*, 7(8), 1218-1239.

Stoeser, D. B., Shock, N., Green, G. N., Dumonceaux, G. M., and Heran, W. D. (2005). "Geologic Map Database of Texas." U. S. Geological Survey Data Series.

Tabari, H., Nikbakht, J., and Hosseinzadeh Talaee, P. (2013). "Hydrological Drought Assessment in Northwestern Iran Based on Streamflow Drought Index (SDI)." *Water Resources Management*, 27(1), 137-151.

Tavakoli, M., and De Smedt, F. (2012). "Impact of Climate Change on Streamflow and Soil Moisture in the Vermilion Basin, Illinois." *Journal of Hydrologic Engineering*, 17(10), 1059-1070.

Trnka, M., Semerádová, D., Eitzinger, J., Dubrovský, M., Wilhite, D., Svoboda, M., Hayes, M., and Žalud, Z. (2003). "Selected Methods of Drought Evaluation in South Moravia and Northern Austria." *Transport of water, chemicals and energy*

in soil-crop atmosphere system, Institude of Hydrology, Slovak Academy of Sciences, Bratislava, Slovakia.
Twedt, T. M., Schaake, J. C., Jr., and Peck, E. L. (1977). "National Weather Service extended streamflow prediction." *Proceedings 45th Western Snow Conference*, Western Snow Conference, Albuquerque, NM, 52-57.
University of Washington (2015). "Calibration." <http://vic.readthedocs.org/en/master/Documentation/Calibration/>. (October, 2015).
USDA (1991). "State Soil Geographic Data Base (STATSGO) Data Users Guide: Miscellaneous Publication Number 1492." S. C. Service, ed. Beltsville, MD.
USGS (2005). "GEOLOGICAL SURVEY OPEN-FILE REPORT 2005-1351. Preliminary Integrated Geologic Map Databases for the United States: Central States: Montana, Wyoming, Colorado, New Mexico, North Dakota, South Dakota, Nebraska, Kansas, Oklahoma, Texas, Iowa, Missouri, Arkansas, and Louisiana." USGS Mineral Resources Program. 1. http://pubs.usgs.gov/of/2005/1351/.
Watkins, D. W., Jr., McKinney, D. C., Lasdon, L. S., Nielsen, S., and Martin, Q. W. (2000). "A scenario-based stochastic programming model for water supplies from the highland lakes." *International Transactions in Operational Research*, 7(3), 211-230.
Wei, W., and Watkins, D. W., Jr. (2011). "Probabilistic streamflow forecasts based on hydrologic persistence and large-scale climate signals in central Texas." *Journal of Hydroinformatics*, 13(4), 760.
Wilhite, D. A. (1992b). "Drought." *Encyclopedia of Earth System Science*, W. A. Nierenberg, ed., Academic Press, Inc., New York, NY, 81-92.
Wilhite, D. A. (1997). "State Actions to Mitigate Drought: Lessons Learned." *Journal of the American Water Resources Association (JAWRA)*, 33(5), 961-968.
Wilhite, D. A., and Glantz, M. H. (1985). "Understanding the Drought Phenomenon: The Role of Definitions." *Water International*, 10(3), 111-120.
Wilhite, D. A., Hayes, M. J., Knutson, C., and Smith, K. H. (2000). "Planning for Drought: Moving from Crisis to Risk Management." *Journal of the American Water Resources Association (JAWRA)*, 36(4), 697-710.
Wood, A. W., and Lettenmaier, D. P. (2006). "A Test Bed for New Seasonal Hydrologic Forecasting Approaches in the Western United States." *Bulletin of the American Meteorological Society*, 87(12), 1699-1712.
Wood, A. W., Maurer, E. P., Kumar, A., and Lettenmaier, D. P. (2002). "Long-range experimental hydrologic forecasting for the eastern United States." *Journal of Geophysical Research*, 107(D20).
Wood, A. W., and Schaake, J. C. (2008). "Correcting Errors in Streamflow Forecast Ensemble Mean and Spread." *Journal of Hydrometeorology*, 9(1), 132-148.
Xue, X., Zhang, K., Hong, Y., Gourley, J. J., Kellogg, W., McPherson, R. A., Wan, Z., and Austin, B. N. (2015). "New Multisite Cascading Calibration Approach for Hydrological Models: Case Study in the Red River Basin Using the VIC Model." *Journal of Hydrologic Engineering*.

Yapo, P. O., Gupta, H. V., and Sorooshian, S. (1998). "Multi-objective global optimization for hydrologic models." *Journal of Hydrology*, 204(1), 83-97.
Zimmerman, B., and Block, P. (2015). "Utilizing the State of ENSO as a Means for Season-Ahead Predictor Selection." *(In review)*.

Appendix A. Steps to Run VIC and Routing Models

The latest versions of the source code for VIC and the routing model are available for download on the University of Washington VIC github webpage at https://github.com/UW-Hydro/VIC. All previous archived versions of VIC are also available. VIC and the routing model have been developed for use in a LINUX/UNIX environment and can be run either using a LINUX operating system, or using Cygwin as a LINUX emulator on a Windows operating system. The models have not been tested using Cygwin, and it is recommended to run VIC and the routing model in a LINUX environment. VIC and the routing model can run in a Bash or C shell in the LINUX terminal.

After downloading the source code, VIC must be compiled with the GNU Compiler Collection (GCC) compiler using the "make" command. Changing directories to the source code, typing "make" will compile VIC using its Makefile and form the vicNl.exe executable file. The same procedure is done for the routing model using the GFortran compiler for the routing source code to form the rout.exe executable file.

In order to run VIC, the proper watershed files must be generated and/or downloaded. The watershed of interest must be delineated and placed on a grid scale. The files required for use in VIC include meteorological forcing files for each grid cell of interest, a soil parameter file to provide soil characteristics per grid cell, a vegetation library file to describe land cover types, and a vegetation parameter file to describe the land cover per grid cell. Optional input files include a watershed state file (which is generated by VIC) to save the state of the water balance at a point in time in order to

restart an analysis at the specified time; an elevation band file to simulate land surface elevations across grid cells; and lake and wetland parameter files for surface water analyses. The directory path names to these files are declared in the global parameter file. The global parameter file also tells VIC the years to simulate, the years that are included in the forcings files, and the output directory name of the generated flux files for each grid cell. Other options, including calculation methods, can be edited in the global parameter file. Descriptions of how to delineate the watershed and how to generate the parameter files are given on the VIC documentation website at http://vic.readthedocs.org/en/master/Documentation/Inputs/.

After the parameter files are generated and the appropriate time frame of analysis is chosen, the VIC model is ready to be run. Changing directories in the terminal to the directory consisting of the vicNl.exe executable, the VIC model is run by typing "vicNl -g <input_global_parameter_file>," where <input_global_parameter_file> is the name of the global parameter file to be used for the simulation. The VIC model will run and compute flux files for each grid cell in the output directory defined in the global parameter file. VIC will print any errors to the standard output and abort. VIC may also list warnings in the standard output, but will continue to run. Output can be viewed in a text editor.

Appropriate input files must also be generated for the routing model. The routing model runs using an input file which gives directory paths to other required inputs. These include a fraction file, which describes the fraction of flows which contribute to the watershed; a flow direction file, which describes the direction water flows between adjacent grid cells; a flow velocity file to describe the velocity of routed flows per grid

cell; a flow diffusion file to assign diffusivity per grid cell; an x-mask file to describe the size of each cell (in meters); a station location file to describe sub-watershed outlets where flows are to be routed; and a unit hydrograph file to describe the impulse response function. The routing model requires the use of a flow direction file and a unit hydrograph file, but the other files are optional. For each category without an input file, a constant value must be assigned in the routing input file. The routing input file also describes the directory for the input flux files generated by VIC, the directory path for the routed output files, and the time frame which the flux files are to be routed. Descriptions of how to generate each input file can be found on the VIC documentation website at http://vic.readthedocs.org/en/master/Documentation/Routing/RoutingInput/.

After creating the appropriate input files and changing directories to the "rout.exe" executable, the routing model is run using the command "route <routing input file>," where <routing input file> is the name of the input file describing the directory names to the necessary input files. The routed flows per station will be written into separate files, named for each station listed in the station file, on both a per month and a per year basis in units of cubic feet per second (cfs) and millimeters of water over the basin.

In order to run the seasonal hindcast model provided in the supplemental materials, open the "01Model" folder in the terminal, type "./code_final.sh", and press "Enter". This will provide output in the "outputrout.txt" file located in the directory, "01Model/route_code/rout_output/output.txt". An already compiled executable of VIC and Rout1.0 are included. Full model components required for compilation can be downloaded at the VIC github webpage at https://github.com/UW-Hydro/VIC.

Appendix B. Grid Cell Aggregation Methods

In order to use the Livneh et al. (2013) meteorological forcings files in the VIC model, the Livneh et al. (2013) forcings needed to be aggregated from a 1/16° scale to a 1/8° scale. To determine the respective coordinates to download from the U.S. Bureau of Reclamation, the 1/8° coordinates of the Lower Colorado River basin had to be disaggregated into 1/16° coordinates for appropriate download links. This was done using the code "latlon.c" available in the VIC model's post-processing tools. This script reads an input mask file to compute the corresponding coordinates of the active cells, and is included in "02External_Scripts" folder in the supplemental materials. The fraction file for the routing model was used as the mask file, and using "latlon.c" to output coordinates on a 1/16° grid, a list of the total basin's grid coordinates was obtained. However, the active cells included the Upper Colorado River basin, and so a script was created to extract only the coordinates for the Lower Colorado River basin. Once the Lower Colorado River basin extent on a 1/16° grid was obtained, these coordinates were then extracted from the U.S. Bureau of Reclamation server. After the appropriate lower basin grid cells were downloaded, they needed to be aggregated to a 1/8° scale. This aggregation was completed using the "aggregate_metdata.c" function available under the VIC model's post-processing tools. Some modifications had to be made to this file in order to aggregate the data appropriately, including adding the correct prefix and directory of the downloaded 1/16° files, aggregating from 5 decimal coordinates to 4 decimal coordinates, and revising the code do an aggregation instead of a disaggregation. This revised file is included in the "02External_Scripts" folder in the supplemental

materials. Aggregation was completed by adding or subtracting 1/32° to the center coordinate of the 1/16° cell in order to aggregate to a 1/8° cell. This process is depicted in Figure B.1.

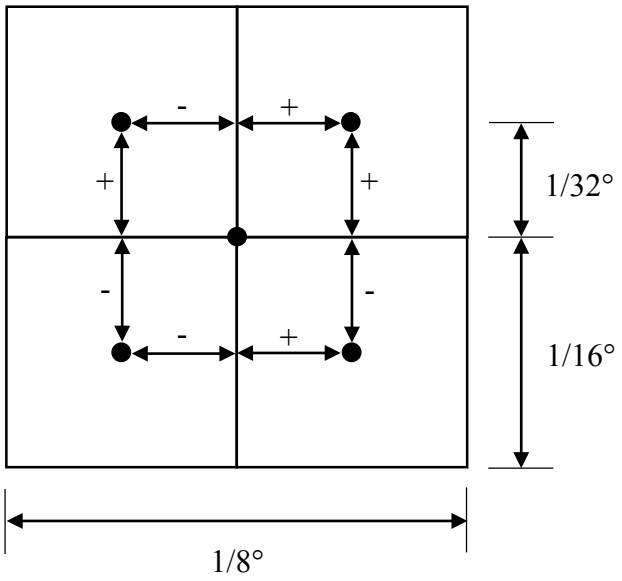

Figure B.1. Disaggregation of a 1/8° cell to four 1/16° cells by adding or subtracting 1/32° to each coordinate. The signs would be opposite for an aggregation of four 1/16° cells to a 1/8° cell.

Appendix C. STATSGO Soil Layer Aggregation

In order to aggregate the STATSGO soil layers into three soil layers, averaged across a 1/8° grid, the soil layers for each spatial polygon (identified as a map unit identification, or MUID) first needed to be separated into three layers. Many map units consisted of three soil layers per sequence number, but other map units consisted of soil layers ranging up to six layers. Afterwards, the difference between the high and low soil depth for each sequence number was computed. Finally, the average of this difference (to compute soil thickness) was computed across the map unit. The following guidelines were used in aggregating soil layers into three layers:

1. As often as possible, utilize the STATSGO defined soil layer breaks.
2. Define soil layers according to large changes in soil texture.
3. If there are four soil layers, combine the fourth layer with the third layer. If there are more than four soil layers, combine the layers with the closest soil textures into one layer.
4. If a sequence number reaches bedrock before another sequence number in the same map unit, the bedrock layer is considered to have a depth of 0 inches for that sequence number. This way, when layer depths are averaged across sequence numbers, bedrock will not be included in the layer.
5. Average depth of the first soil layer must be less than the average depth of the second soil layer. In the case where the first and second soil layers could not be defined by texture, and the first soil layer depth is greater

than the second soil layer depth, then the average of the two layers was taken and applied to both layers (example: soil layer 1 = 22 in., soil layer 2 = 11 in., then both soil layers would be given a value of 17 in.).

A list of map units needing to be averaged into three soil layers is given in Table C.1. The table also describes which soil layers were aggregated according to the guidelines above to make three soil layers applicable to use in the VIC model.

Spatially weighted averages of soil depth were then applied to the 1/8° grid of the Lower Colorado River watershed. This spatially weighted average was taken by multiplying the area of the grid cell by the average layer depth for each of the three soil layers. The grid cells along the border of the Lower Colorado River basin contribute fractional areas to the basin in terms of runoff. This technique assumes the soil layer variability over the map unit, averaged together into three soil layers, applies to the fraction of the grid cell, which could result in biased results in the spatial variability of soil depth for the border grid cells.

Table C.1. Aggregation of STATSGO Soil Layers to Three Soil Layers to use in VIC.

MUID	VIC Soil Layer	STATSGO Soil Layers to form VIC Soil Layer
TX061	1	1
	2	2
	3	3 - 6
TX070	1	1
	2	2
	3	3 - 5
TX087	1	1
	2	2
	3	3 - 5
TX089	1	1
	2	2
	3	3 - 5
TX095	1	1
	2	2 - 3
	3	4
TX105	1	1
	2	2
	3	3 - 6
TX119	1	1
	2	2 - all but last component of 3
	3	Last component of 3 - 5
TX121	1	1
	2	2 - 3
	3	4 - 5
TX137	1	1
	2	2
	3	3 - 6
TX144	1	1
	2	2
	3	3 - 6
TX153	1	1
	2	All but last six components of 2
	3	Last six components of 2 - 6
TX155	1	1

	2	2 - 3
	3	4 - 6
TX161	1	1
	2	2 - all but last four components of 3
	3	Last four components of 3 - 5
TX169	1	1, then depth averaged with Layer 2 so equals Layer 2 depth
	2	2 - 3, then depth averaged with Layer 2 so equals Layer 2 depth
	3	4
TX187	1	1
	2	2
	3	3 - 4
TX188	1	1
	2	2
	3	3 - 5
TX192	1	1
	2	2
	3	3 - 4
TX210	1	1
	2	2
	3	3 - 5
TX214	1	1
	2	2 - 3
	3	4
TX227	1	1
	2	2
	3	3 - 5
TX252	1	1 - 2
	2	3
	3	4
TX253	1	All but last three components of 1
	2	Last three components of 1 - all but last two components of 2

	3	Last two components of 2 - 3
TX257	1	1
	2	2 - all but last two components of 4
	3	Last two components of 4 - 5
TX273	1	1
	2	2
	3	3 - 6
TX295	1	1
	2	2
	3	3 - 5
TX301	1	1
	2	2 - last two components of 3
	3	Last two components of 3 - 5
TX309	1	1
	2	2
	3	3 - 6
TX310	1	1
	2	2 - 3
	3	4
TX318	1	1
	2	2 - 3
	3	4 - 5
TX329	1	1
	2	2 - 3
	3	4
TX360	1	1
	2	2
	3	3 - 5
TX362	1	1
	2	2
	3	3 - 5
TX371	1	1
	2	All but last two components of 2
	3	Last two components of 2 - 6

TX380	1	All but last two components of 1
	2	Last two components of 1 - 2
	3	3 - 4
TX442	1	1
	2	2
	3	3 - 6
TX454	1	1
	2	2 - 3
	3	4 - 5
TX481	1	1 - 2
	2	3
	3	4 - 5
TX484	1	1
	2	2 - 3
	3	4
TX488	1	1
	2	2
	3	3 - 5
TX520	1	1
	2	2
	3	3 - 5
TX521	1	1
	2	2 - 3
	3	4 - 6
TX526	1	1
	2	2 - 3
	3	4
TX539	1	1
	2	2
	3	3 - 4
TX542	1	1
	2	2
	3	3 - 6
TX543	1	1 - 2
	2	3
	3	4 - 5
TX545	1	1
	2	2
	3	3 - 6

TX546	1	1
	2	2
	3	3 - 6
TX553	1	1
	2	2 - 3
	3	4 - 5
TX555	1	1
	2	2
	3	3 - 5
TX565	1	1, then depth averaged with Layer 2 so equals Layer 2 depth
	2	2, then depth averaged with Layer 1 so equals Layer 1 depth
	3	3 - 4
TX592	1	1
	2	2
	3	3 - 5
TX598	1	1
	2	2
	3	3 - 4
TX609	1	1
	2	2
	3	3 - 5
TX615	1	1
	2	2 - 3
	3	4
TX617	1	1
	2	2 - 3
	3	4
TX626	1	1
	2	2 - 3
	3	4 - 5

Appendix D. Grid Cell Coordinates

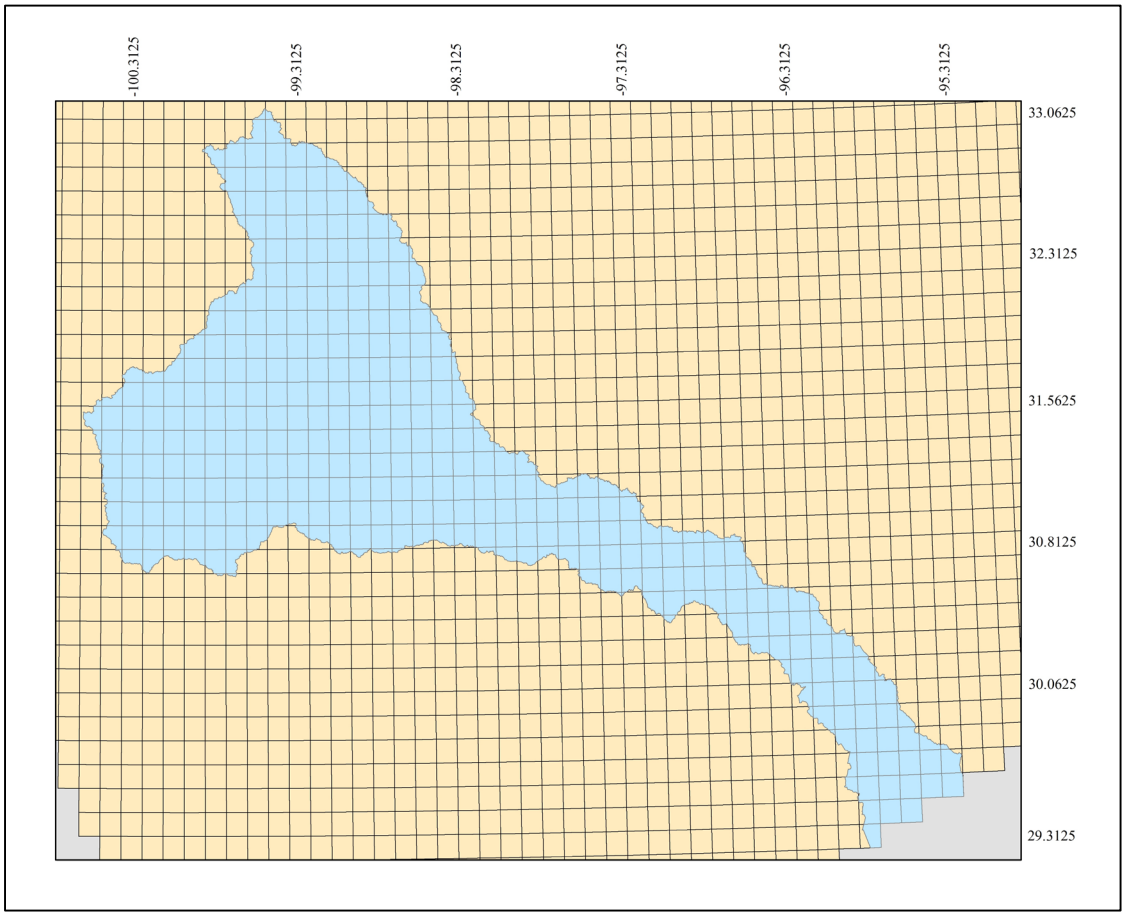

Figure D.1.Grid Cell Coordinates of the Lower Colorado River Basin. Latitudinal coordinates are °N, and longitudinal coordinates are °E. (Figure by author).

The three grid cells with coordinates of (30.9375° N, -100.5625° E); (31.0625° N, -100.4374° E); and (31.0625° N, -100.3125° E) are included in the lower basin watershed extent, but have flow direction values which do not contribute flows through the basin. These cells have meteorological forcings files, and are included in the soil parameter file, vegetation parameter file, snow band parameter file, fraction file, and flow direction file because they are included in the basin.

In the extreme western boundary of the basin, the grid cell coordinates (30.4375° N, -100.5625° E) and (30.5635° N, -100.5625° E) are missing from the download of the South Central (Gulf) watershed region, but are included in the Lower Colorado River basin extent. Downloads of meteorological forcing files list these two grid cell coordinates in the Rio Grande watershed dataset. Since the areas of these two grid cells of the watershed are very small at 0.021 km^2 for coordinate (30.4375° N, -100.5625° E) and 4.015 km^2 for coordinate (30.5625° N, -100.5625° E), it is assumed the streamflow contribution from these cells is negligible. This resulted in a total of 397 forcing files to be considered for the Lower Colorado River basin extent.

The Livneh et al. (2013) forcings were lacking twenty 1/16° grid cells available for download, equivalent to five 1/8° grid cells after aggregation. These five grid cells were located on the southeastern edge of the basin, along the Gulf of Mexico, and therefore the routed water from these cells would not be considered in routing to stations CRBU and CRTR. Nearby 1/8° cells were used to estimate the missing grid cells. The nearby 1/8° cells were disaggregated using the "aggregate_metdata.c" script into four 1/16° cells. These 1/16° cells were then used to estimate the missing grid cells from Livneh et al. (2013). Once the 1/16° cells were estimated, they were aggregated back to

the 1/8° extent. The list of missing grid cell coordinates and the grid cells assumed containing similar data for the missing cells are listed in Table D.1.

Table D.1. Estimated Grid Cell Coordinates for Aggregation. Coordinates are listed as (°N, °E).

Use		To Estimate	
1/8°	1/16°	1/16°	1/8°
28.8125, -95.5625	28.84375, -95.59375	28.84375, -95.46875	28.8125, -95.4375
	28.84375, -95.53125	28.84375, -95.40625	
	28.78125, -95.59375	28.78125, -95.46875	
	28.78125, -95.53125	28.78125, -95.40625	
28.8125, -95.6875	28.84375, -95.71875	28.71875, -95.71875	28.6875, -95.6875
	28.84375, -95.65625	28.71875, -95.65625	
	28.78125, -95.71875	28.65625, -95.71875	
	28.78125, -95.65625	28.65625, -95.65625	
28.8125, -95.8125	28.84375, -95.84375	28.71875, -95.84375	28.6875, -95.8125
	28.84375, -95.78125	28.71875, -95.78125	
	28.78125, -95.84375	28.65625, -95.84375	
	28.78125, -95.78125	28.65625, -95.78125	
28.8125, -95.9375	28.84375, -95.96875	28.71875, -95.96875	28.6875, -95.9375
	28.84375, -95.90625	28.71875, -95.90625	
	28.78125, -95.96875	28.65625, -95.96875	
	28.78125, -95.90625	28.65625, -95.90625	
28.6875, -96.0625	28.71875, -96.09375	28.59375, -95.96875	28.5625, -95.9375
	28.71875, -96.03125	28.59375, -95.90625	
	28.65625, -96.09375	28.53125, -95.96875	
	28.65625, -96.03125	28.53125, -95.90625	

Appendix E. Complete Calibration Methods and Results

To calibrate the VIC model, the soil parameters b_{infilt}, Ds, Ds_{max}, Ws, and the three layers of soil depth were chosen for calibration (see section 4.2). First, the upper and lower bounds of each calibrated parameter were assessed following guidelines from the University of Washington (see section 4.4). In order to apply the SRTC calibration tool, the low and high bounds of each parameter needed to be scaled from 0 to 100. The low bound was assigned a value of 0; the initial value from the NLDAS dataset used in the study conducted by CH2M HILL (2008) was assigned a value of 50; and the upper bound was assigned a value of 100. Then, multipliers were calculated to represent the percentage of change from the initial parameter of 50 if the value were varied from 0 to 100. The value of 50 is assigned a multiplier of 1, signifying that multiplying the initial value by 1 would result in no change for the parameter in the SRTC tool. The multipliers were calculated by assuming a linear relationship in the scaling from 0 to 50, and from 50 to 100. The difference between the initial value and the extremity is taken and is divided into 50 parts for scaling. This represents the increase (or decrease) in the scaling factor for every one increase (or decrease) in the scale.

For example, for the parameter of b_{infilt}, the low bound is 0.5. The lowest value in the original soil input file from the NLDAS dataset (CH2M HILL 2008) is 0.96; therefore, in order to reach this low bound, the smallest allowable multiplier would be 0.53, while maintaining multipliers to two decimal places for the extremes.

Original value * Multiplier = Low Bound

0.96 * 0.53 = 0.5088

Therefore, the multiplier of 0.53 would correspond to the value of 0 on a scale from 0 to 100. Since the value of 50 refers to a multiplier of 1, the difference between these multipliers can be divided into 50 equal intervals:

$$\frac{\text{Multiplier for value 50 - Multiplier for value 0}}{50} = \frac{1 - 0.53}{50} = 0.0094$$

Therefore, for every unit value added between 0 and 50, the multiplier increases by 0.0094.

Multiplier for Previous Value + Multiplier per Value = Multiplier for + 1 Unit Value

Since the multiplier for a scale value of 0 is 0.53, the new multiplier for the scale value of 1 is 0.5394.

A similar technique was used for scaling between 0 and 100, but since the high bound is different than the low bound, the scaled multiplier for each unit increase between 50 and 100 is different than between 0 and 50.

In order to convert the multiplier to a percent change, the multiplier was subtracted from (or added to) 1 and multiplied by 100 to determine the percent decrease (or increase). For example, for a reduction in the percent decrease of b_{infilt} from a scale value of 50 (the original value) to a scale value of 1, the percent decrease is:

$$(1 - 0.5394) * 100\% = 46.06\%$$

The VIC model was run using a soil file where each individual parameter was decreased to the low bound as well as increased to the high bound to determine the minimum and maximum flows the parameter produces if all other parameters were left at their initial values from the CH2M HILL (2008) study. The calibrated values are then calculated according to equation (4.4). The weights in equation (4.4) range from -1 to 1,

where -1 refers to a scale value of 0, 0 refers to a scale value of 50, and 1 refers to a scale value of 100.

The SRTC was applied twice, once to route flows to the CRBU station and again to route flows within the incremental sub-basin of CRTR-CRBU. A non-linear optimization algorithm was used to maximize the (approximated) NSE, subject to the constraints that the scale value for each parameter must range between 0 and 100 (see section 4.4). Although a multi-start technique was implemented, starting values of 0, 50, and 100 for all parameters were used to help ensure the global maximum NSE was found. The SRTC initially calibrated values for each parameter for the full time period; then, after verification, the SRTC was used for both sub-basins for the period 1960 through 1989. Calibrated ranges of parameters for the entire Lower Colorado River basin are given in Table E.1. Flow comparisons to the LCRA observed inflows for the CRBU and CRTR-CRBU basins are provided in Figures E.1 and E.2, respectively. Verification results utilizing these calibrated estimates in VIC are presented in Table 4.3.

Table E.1. SRTC Calibration of Soil Parameters.

Parameter	Original Range	Calibrated Range (1940-2011)	Calibrated Range (1960-1989)*
b_{infilt}	0.01 – 0.50	0.01 – 0.50	0.01 – 0.50
Ds	0.0001 – 0.0050	0.0001 – 0.1145	0.0001 – 0.6397
Ds_{max}	10 (unvaried)	10 (unvaried)	6.9 – 10
Ws	0.96 – 1	0.888 – 1	0.888 – 1
Soil Layer 1	0.0101 – 0.5122	0.0101 – 0.5122	0.0101 – 0.5122
Soil Layer 2	0.0423 – 1.082	0.0423 – 1.082	0.0423 – 1.082
Soil Layer 3	0.0290 – 1.443	0.0290 – 1.244	0.0290 – 1.244

*The ranges presented for the 1960-1989 calibration were computed using the verification of the 1940-2011 calibration, with the soil parameter ranges presented updated from the 1940-2011 calibrated ranges.

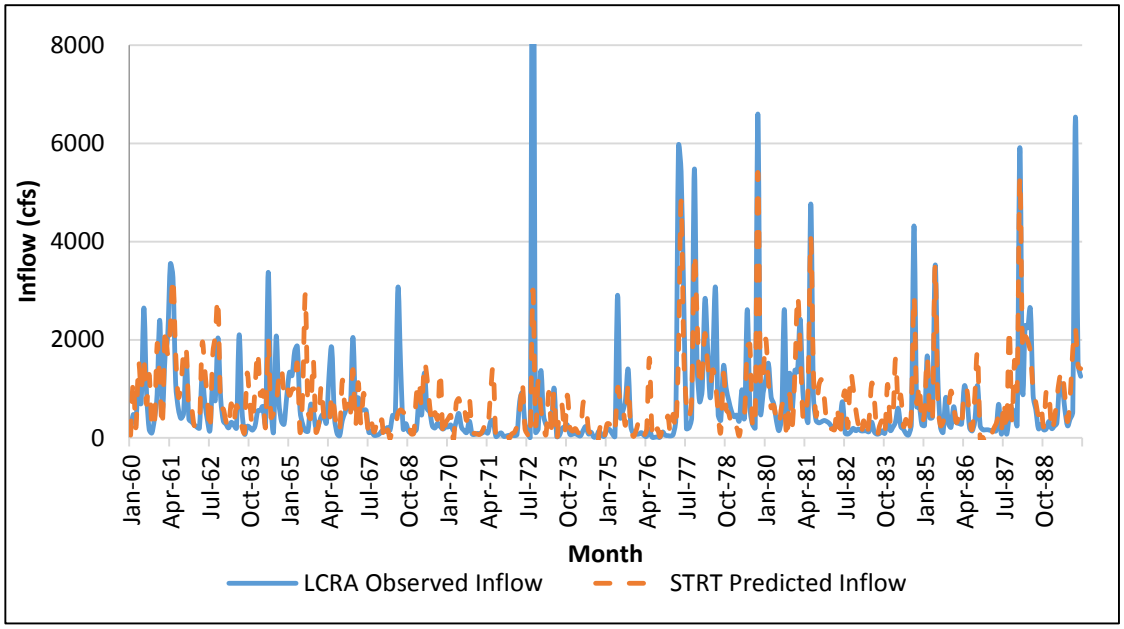

Figure E.1. SRTC Calibrated Flows for a Verification Period of 1960-1989 for the CRBU basin. Created by author.

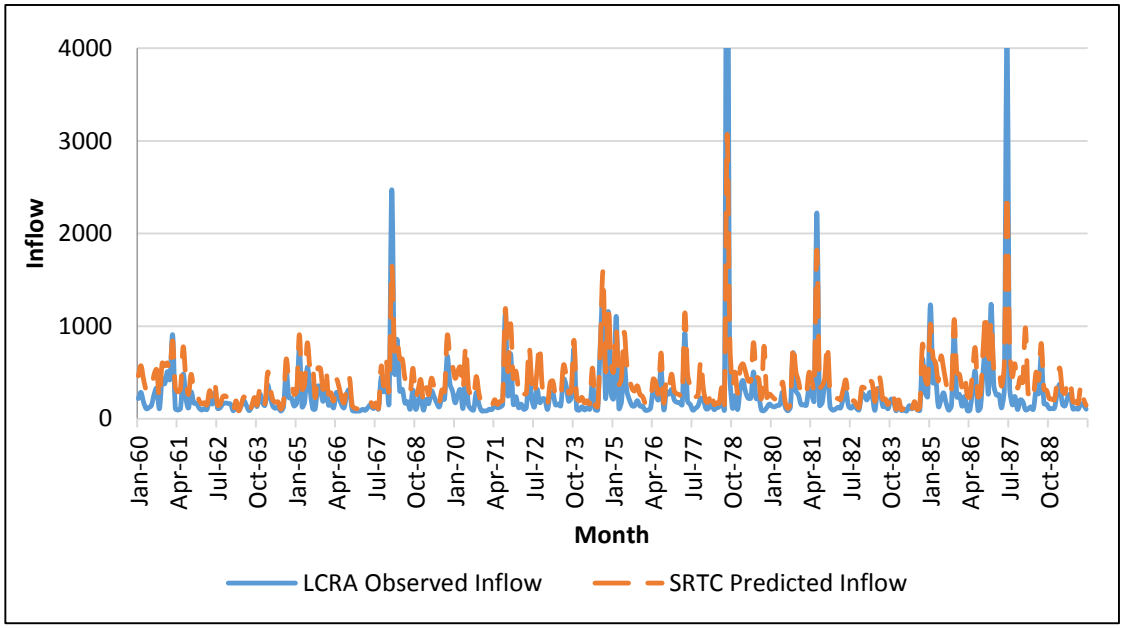

Figure E.2. SRTC Calibrated Flows for a Verification Period of 1960-1989 for the CRTR-CRBU basin. Created by author.

Since the calibration procedure was analyzed by decade rather than season, a continuous run of the VIC model from 1960 through 2011 was completed. To support the model calibration, the historical data were also run through the calibrated model on a seasonal basis, with the watershed "state" saved before each season as done for the hindcasting procedure and compared to the LCRA observed inflows. High r^2 values of 0.827 and 0.764 for the MAMJ and JASO seasons, respectively, support the model is calibrated accurately. Scatterplots representing the seasonal historical data compared to the LCRA observed inflows are given in Figures E.3 and E.4.

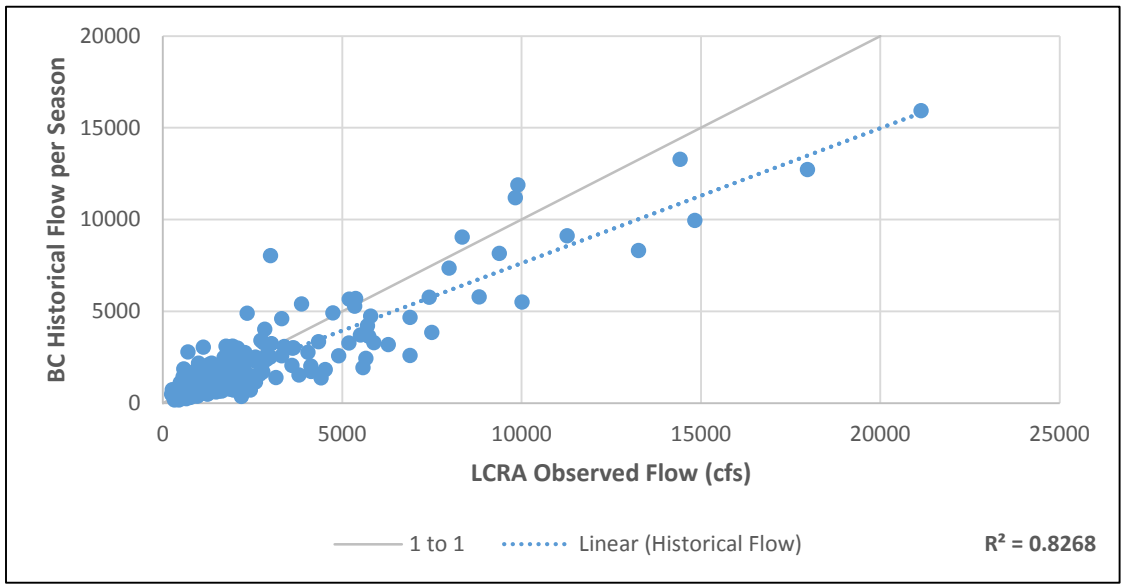

Figure E.3. VIC Simulated Flows using Historical Data for the MAMJ Season, 1960-2011. Created by author.

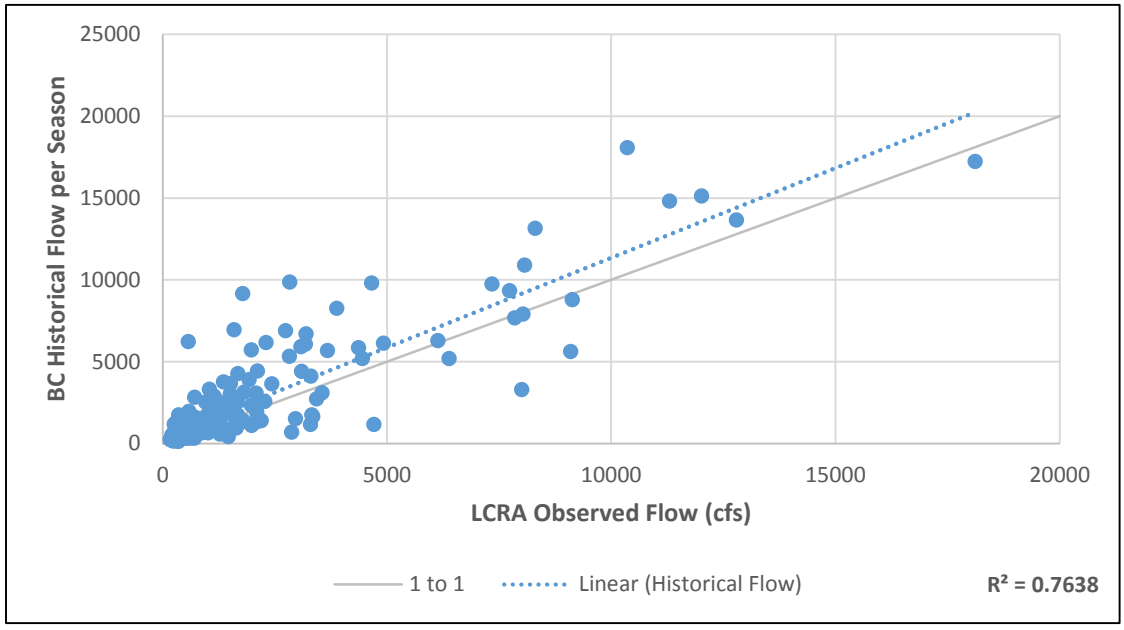

Figure E.4. VIC Simulated Flows using Historical Data for the JASO Season, 1960-2011. Created by author.

Appendix F. Bias Correction Technique

A percentile matching procedure was applied as a bias correction technique during the verification and hindcast modeling stages to eliminate bias in the simulated results. This technique is used frequently in hydroclimatic studies, and has been used with VIC forecast models (Wood and Lettenmaier 2006; Wood et al. 2002; Wood and Schaake 2008). In this study, the technique matched streamflow percentiles of hindcasts to LCRA observed inflows. First, a cumulative distribution function was created to calculate the percentile of the flow rank in relation to the simulated flow dataset. Then, the percentile was matched to the cumulative distribution function percentile of the LCRA's observed inflows (or the historical simulated flows); this assumes the simulated and observed flows follow a normal distribution. The ensemble mean flows are then corrected to the percentile of the observed (or historical simulated) flows. Afterward, the percent bias for each decade (during the verification stage) or each season (during the hindcast stage) was calculated using equation (4.3). While the bias is significant in some decades, the bias correction procedure ensures that the overall bias (across the entire time series) is very close to zero. An example of the percentile matching across the cumulative distribution functions of the simulated flows and the observed flows for 1960 through 2010 is presented in Figure F.1.

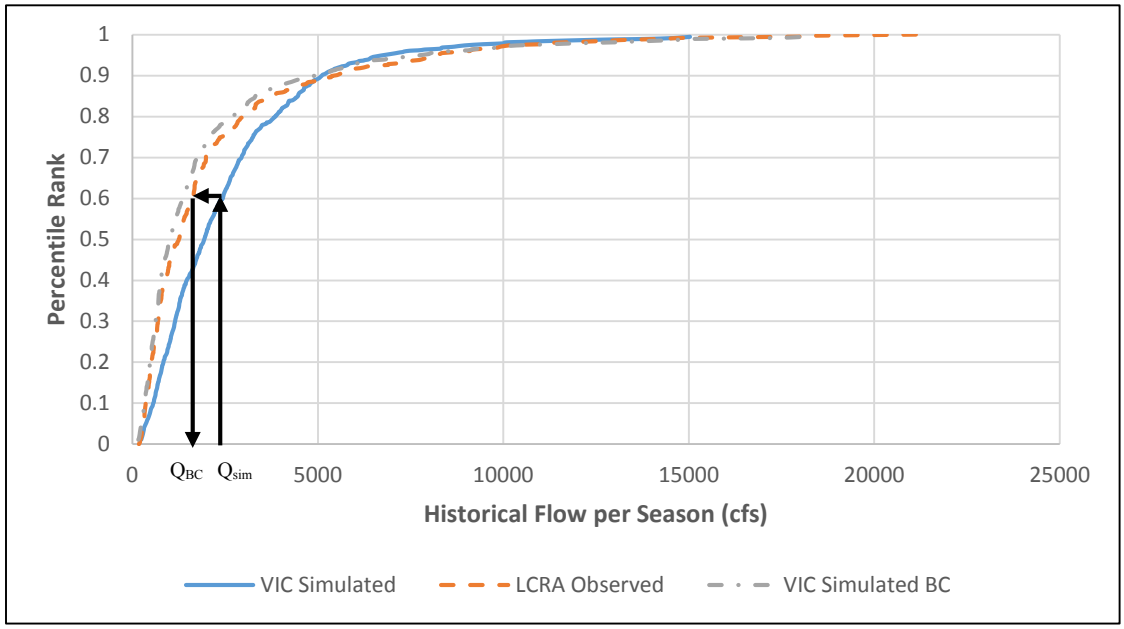

Figure F.1. Cumulative Distribution Function of Percentile Matching Bias Correction Procedure, showing a bias corrected flow for matching a percentile of 0.6. Created by author.

Appendix G. Hindcasting Procedure

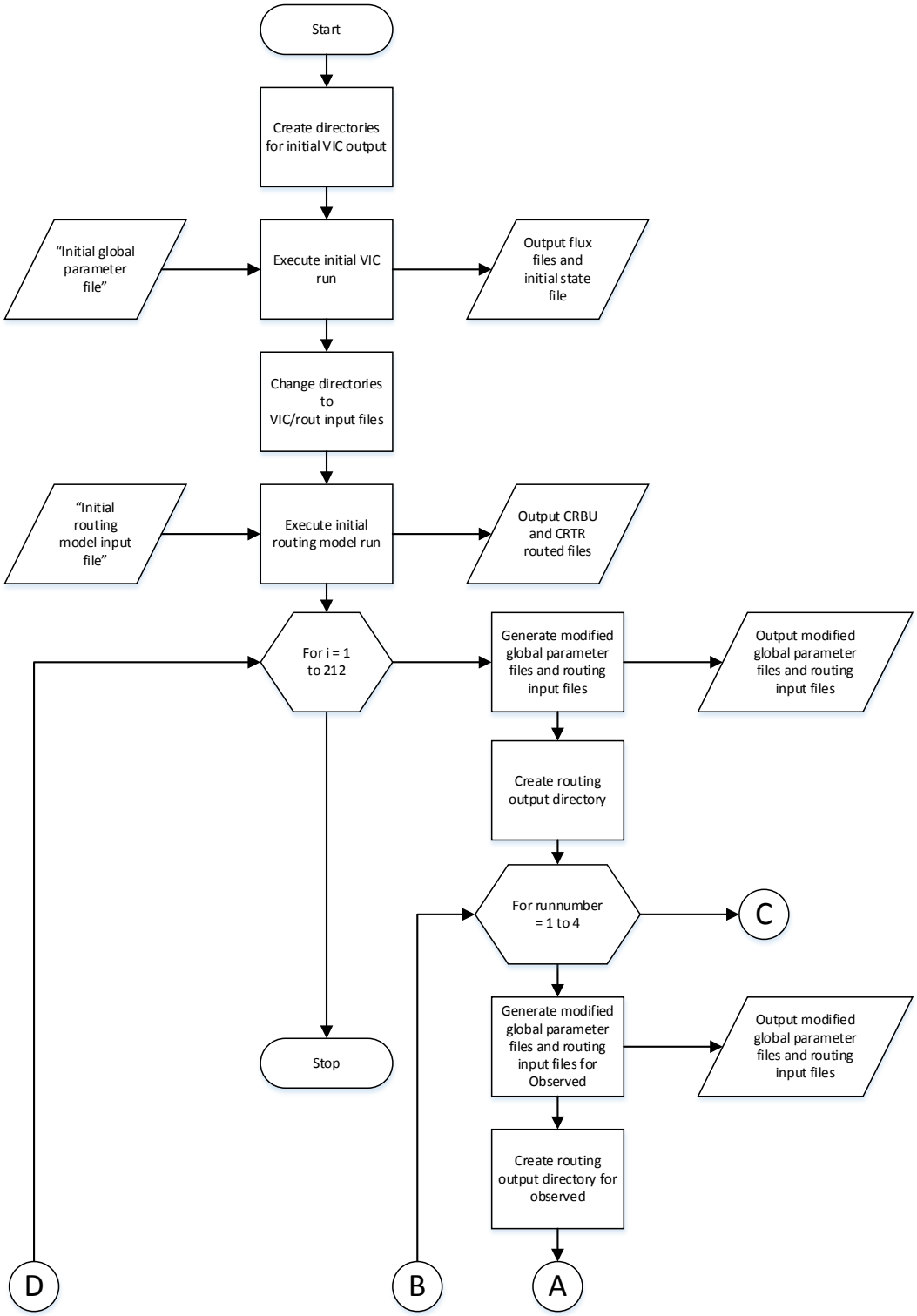

Figure G.1. Seasonal Hindcast Procedure

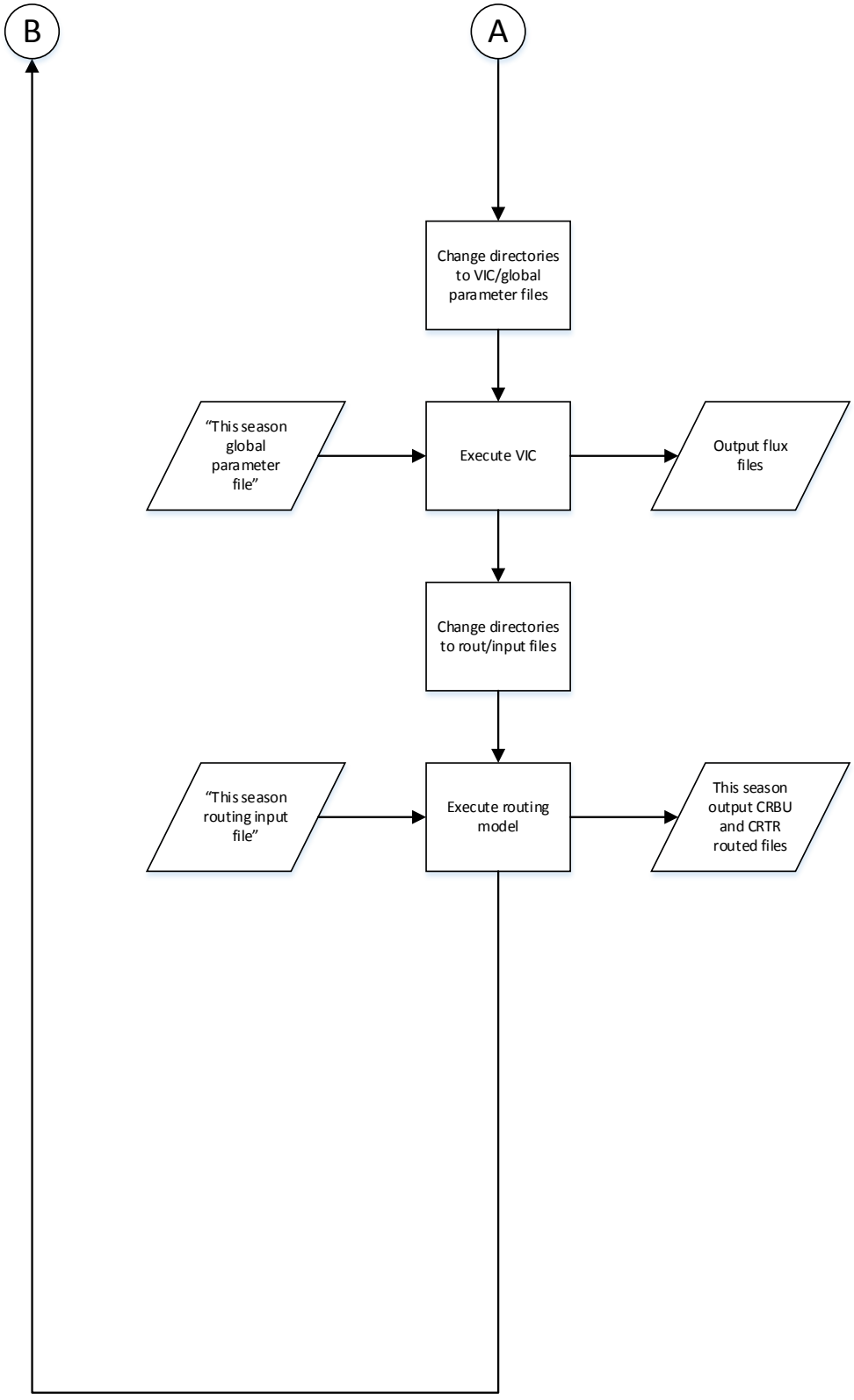

Figure G.1 (continued). Seasonal Hindcast Procedure

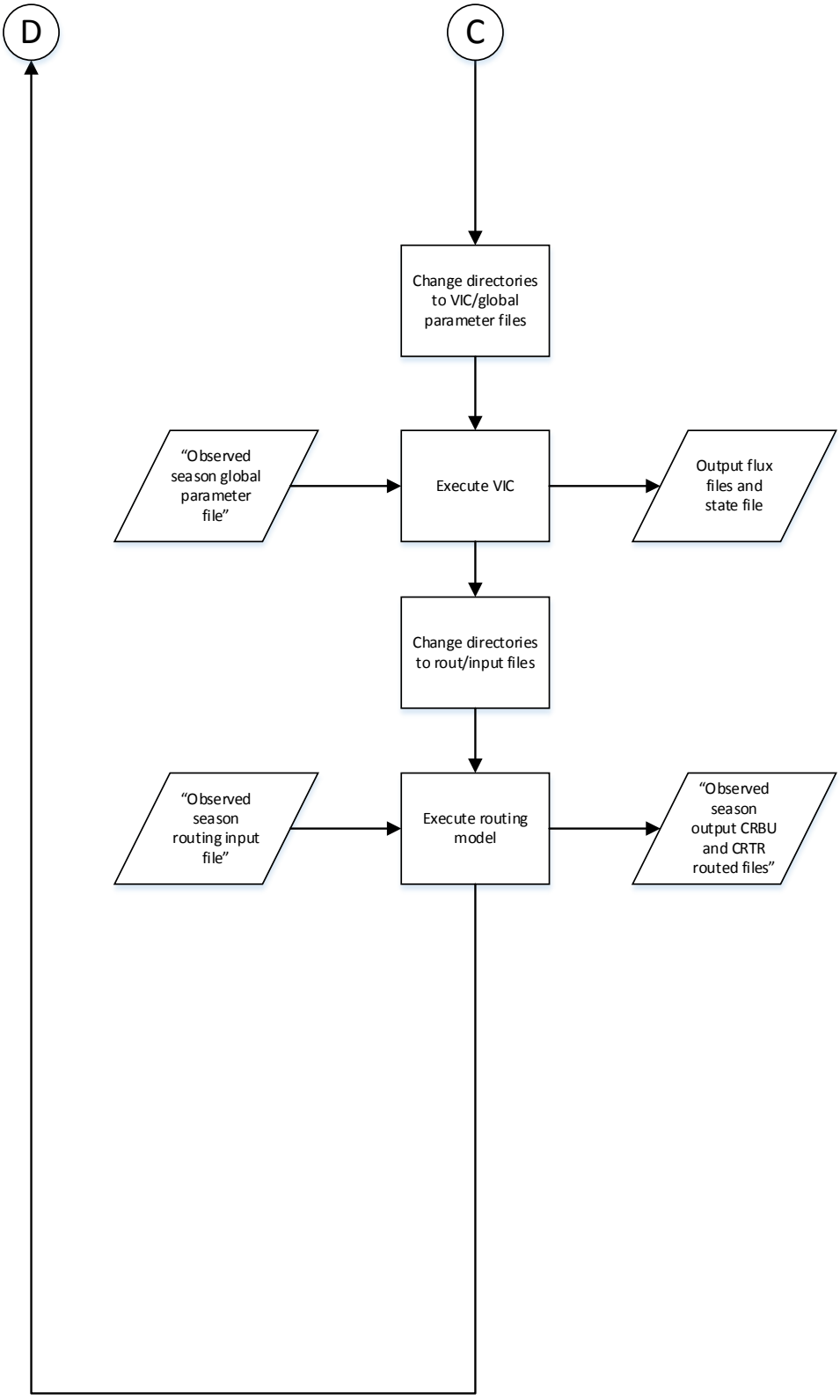

Figure G.1 (continued). Seasonal Hindcast Procedure

Appendix H. Example of Analog Year Selection

Table H.1. Analog Year Predictions for MAMJ. Generated by Brian Zimmerman, University of Wisconsin Madison.

Year to be Modeled	Analog Years									
1960	1966	1936	1931	1993	1980	1951	1921	1961	1930	1991
1961	1951	1937	1962	1927	1980	1936	1931	1966	1924	1928
1962	1961	1966	1989	1959	1991	1936	1973	1980	1921	1970
1963	1961	1989	1991	1973	1970	1966	1980	1945	1924	1938
1964	1944	1945	1954	1970	1955	1947	1952	1958	1985	1946
1965	1965	1968	1986	1932	1975	1979	1949	1926	1940	1921
1966	1966	1936	1961	1980	1989	1991	1993	1931	1921	1973
1967	1921	1932	1959	1966	1993	1936	1979	1961	1989	1965
1968	1940	1949	1968	1986	1982	1979	1926	1932	1965	1987
1969	1989	1961	1991	1973	1970	1945	1954	1980	1938	1924
1970	1970	1958	1945	1954	1973	1985	1929	1990	1991	1989
1971	1978	1925	1962	1996	1928	1971	1927	1951	1937	1974
1972	1959	1921	1932	1966	1936	1961	1993	1989	1979	1991
1973	1961	1959	1989	1991	1973	1929	1970	1966	1990	1980
1974	1996	1928	1978	1925	1974	1927	1971	1962	1948	1937
1975	1979	1959	1932	1982	1969	1949	1986	1929	1968	1990
1976	1962	1951	1963	1931	1927	1934	1978	1925	1928	1930
1977	1977	1990	1985	1958	1929	1969	1995	1970	1959	1942
1978	1931	1963	1930	1951	1993	1936	1966	1921	1980	1962
1979	1966	1961	1991	1989	1980	1973	1936	1924	1970	1937
1980	1966	1936	1993	1921	1931	1980	1961	1989	1991	1951
1981	1959	1979	1969	1929	1932	1990	1982	1961	1989	1949
1982	1958	1985	1990	1929	1977	1970	1944	1945	1973	1989
1983	1939	1967	1933	1934	1943	1972	1950	1983	1960	1963
1984	1971	1974	1996	1948	1984	1925	1953	1978	1964	1956
1985	1991	1973	1989	1961	1970	1945	1980	1954	1938	1924
1986	1959	1932	1979	1961	1989	1966	1921	1929	1991	1936
1987	1982	1949	1940	1986	1968	1979	1932	1969	1987	1959
1988	1947	1944	1946	1988	2003	1994	1955	1985	1958	1945
1989	1985	1958	1990	1929	1944	1970	1947	1945	1954	2003
1990	1958	1985	1990	1929	1970	1945	1944	1973	1954	1989
1991	1938	1954	1924	1945	1952	1973	1970	1991	1980	1937

1992	1979	1932	1959	1986	1982	1921	1949	1965	1968	1961
1993	1993	1930	1931	1921	1963	1936	1923	1966	1951	1950
1994	1985	1958	1990	1929	1970	1944	1945	1977	1954	1973
1995	1995	1977	1969	1981	1990	1922	1985	1958	1929	2009
1996	1955	1952	1946	1948	1938	1944	1954	1988	1924	1945
1997	1995	1969	1977	1922	1987	1982	1981	1935	1990	1949
1998	1948	1974	1928	1996	1927	1978	1962	1925	1953	1971
1999	2009	1942	1977	1985	1958	2003	1990	1995	1994	1929
2000	2009	1942	2003	1994	1985	1958	1977	1947	1944	1990
2001	1953	1964	1984	1998	1948	2005	1974	1988	1946	1955
2002	2005	1988	1994	2003	1947	1998	1946	1944	1964	1942
2003	1941	1981	2004	1922	1995	1935	1999	1977	1987	1969
2004	2004	1999	2000	1941	1981	2009	1995	1977	1942	1922
2005	2001	2002	2006	1998	2008	2005	2010	1994	2003	1988
2006	1998	2005	1988	2002	1964	1994	1953	2006	1946	2003
2007	2004	1941	1999	1981	2000	2007	1922	1995	2009	1935
2008	2009	1999	2000	1942	2003	1994	2006	2002	1947	1985
2009	2002	2006	2001	2005	1998	1994	2003	1942	2009	1988
2010	1999	2009	2000	2004	1942	1977	1995	1981	2003	1985